



UNITED NATIONS
UNIVERSITY

GEOHERMAL TRAINING PROGRAMME
Orkustofnun, Grensásvegur 9,
IS-108 Reykjavík, Iceland

Reports 2008
Number 4

OPEN HEAT EXCHANGER FOR IMPROVED ENERGY EFFICIENCY IN THE HEATING OF HOT SPAS

MSc thesis

Department of Mechanical and Industrial Engineering
University of Iceland

by

Saeid Jalili Nasrabadi

SUNA – Renewable Energy Organization of Iran
Yadegare Emam Highway, Poonake Bakhtari Ave.
Sharake Ghods, P.O. Box 14155-6398

Tehran

IRAN

jalilina@yahoo.com

United Nations University
Geothermal Training Programme
Reykjavík, Iceland
Published in December 2008

ISBN 978-9979-68-250-9

ISSN 1670-7427

This MSc thesis has also been published in July 2008 by the
Faculty of Engineering – Department of Mechanical and Industrial Engineering,
University of Iceland

INTRODUCTION

The Geothermal Training Programme of the United Nations University (UNU) has operated in Iceland since 1979 with six month annual courses for professionals from developing countries. The aim is to assist developing countries with significant geothermal potential to build up groups of specialists that cover most aspects of geothermal exploration and development. During 1979-2008, 402 scientists and engineers from 43 countries have completed the six month courses. They have come from Asia (44%), Africa (26%), Central America (15%), and Central and Eastern Europe (15%). There is a steady flow of requests from all over the world for the six month training and we can only meet a portion of the requests. Most of the trainees are awarded UNU Fellowships financed by the UNU and the Government of Iceland.

Candidates for the six month specialized training must have at least a BSc degree and a minimum of one year practical experience in geothermal work in their home countries prior to the training. Many of our trainees have already completed their MSc or PhD degrees when they come to Iceland, but several excellent students have made requests to come again to Iceland for a higher academic degree. In 1999, it was decided to start admitting UNU Fellows to continue their studies and study for MSc degrees in geothermal science or engineering in co-operation with the University of Iceland. An agreement to this effect was signed with the University of Iceland. The six month studies at the UNU Geothermal Training Programme form a part of the graduate programme. Six UNU-GTP MSc Fellows completed their MSc degree in 2008, the biggest group to date.

It is a pleasure to introduce the fourteenth UNU Fellow to complete the MSc studies at the University of Iceland under the co-operation agreement. Mr. Saeid Jalili Nasrabadi, BSc in Civil Engineering from the Mohaghegh Ardebili University in Iran, of SUNA – Renewable Energy Organization of Iran, completed the six month specialized training in Geothermal Utilization at the UNU Geothermal Training Programme in October 2004. His research report was entitled “Geothermal district heating and swimming pool in the Sabalan area, Iran”. Two years later, in September 2006, he came back to Iceland for MSc studies in Mechanical Engineering at the Department of Mechanical and Industrial Engineering within the Faculty of Engineering of the University of Iceland. In June 2008, he defended his MSc thesis presented here, entitled “Open heat exchanger for improved energy efficiency in the heating of hot spas”. His studies in Iceland were financed by a fellowship from the Government of Iceland through the UNU Geothermal Training Programme. We congratulate Mr. Saeid Jalili Nasrabadi on his achievements and wish him all the best for the future. We thank the Department of Mechanical and Industrial Engineering of the University of Iceland for the co-operation, and his supervisors for the dedication.

Finally, I would like to mention that Saeid’s MSc thesis with the figures in colour is available for downloading on our website at page www.unugtp.is/yearbook/2008.

With warmest wishes from Iceland,

Ingvar B. Fridleifsson, director
United Nations University
Geothermal Training Programme

ACKNOWLEDGEMENTS

I am grateful to The Government of Iceland and Dr. Ingvar Birgir Fridleifsson, Director of the United Nations University - Geothermal Training Programme and the deputy director, Mr. Lúdvík S. Georgsson, for the UNU-GTP MSc Fellowship.

Special thanks to Dr Guðrún Saevarsdóttir and Dr Halldór Pálsson, from University of Iceland, for their supervision, patience, guidance, and advices. I wish to express my appreciation to Professor Páll Valdimarsson, for his excellent support, lectures and his evaluation of the thesis as the external examiner.

Contributions of the Orkusjóður (Energy Fund) of Orkustofnun, Reykjavik Energy and NORM-X HF Company in the project, are gratefully appreciated.

I am grateful to the UNU-GTP staff, Ms. Thórhildur Ísberg, Ms. Dorthe H. Holm and Mr. Markus A. G. Wilde for their continuous help during my stay in Iceland.

I also would like to extend my appreciation to the parents of Guðrún Saevarsdóttir for allowing me to install a project experiment at their home and having me through months. Mr. Vilhjálmur Sigurjónsson from University of Iceland and staff members from Norm-x Company were also very helpful for experiments, their assistance is gratefully appreciated.

Thanks to the entire staff of Orkustofnun and Iceland GeoSurvey - ISOR for their help in many ways. I am indebted to the teachers at the University of Iceland for sharing a great learning experience and a high level of presentation.

Last but not least, my deepest thanks to my family for their help, continuous support and encouragement. I dedicate this work to members of my family and friends who gave me spiritual inspiration during my stay in Iceland. I say thank you so much and god bless you all.

ABSTRACT

Hot spas and Jacuzzis are popular in Iceland due to the abundance of reasonably prized geothermal heat available. However the water from the district heating system is too warm to be admitted directly into the spa. For safety reasons the water is mixed with cold water, from 75 down to 50°C, which leads to wasting a large quantity of heat. Therefore a design was suggested that enables the feeding of geothermal water directly into the pot, omitting the step of mixing it with cold water. The idea is to employ an open heat exchanger that transfers much heat from the geothermal water to the bulk water in the spa, before letting it mix with the spa water. A case study was done for one particular spa. Heat load was calculated and measured when the spa was in use, and when it was unused. A design is suggested employing a circular double-plate which is to be placed at bottom of pot. This unit will function as an open heat exchanger feeding district heating water into the pot. Free convection takes place at the up side of the upper plate and forced convection below the upper plate. Heat transfer coefficient for both was calculated. Temperature field in the pool before and after implementation of the open heat exchanger was measured at different points using thermocouples. The measured temperatures were compared to thermal and fluid-dynamic simulation of the temperature and flow fields obtaining good accordance. Results are reasonable and promising for a good design that may considerably reduce the energy expenses for a continuously heated geothermal spa. More detailed measurements were made on the upper plate of the heat exchanger and detailed simulation of the heat exchanger itself was then used to obtain a value for the heat transfer coefficient for the upper plate to the surrounding water. This information was used to make an improved design for the open plate heat exchanger, stating that a diameter of 63 cm and a thickness of 1.5 cm were suggested as final design. Due to economy consideration the recovery time of the implementing of suggested heat exchanger is estimated to 8 months in studied case.

TABLE OF CONTENTS

	Page
1. INTRODUCTION	1
1.1 Hot pot 1	1
1.2 Previous work and background	2
1.2.1 Free convection from horizontal plates, isothermal surfaces.....	2
1.2.2 Forced convection.....	4
2. METHODOLOGY AND DESIGN	6
2.1 Introduction	6
2.2 Close loop heat exchanger.....	6
2.2.1 Heat loss from pot.....	7
2.3 Manual mixing of cold and hot water	10
2.4 Open heat exchanger	10
2.4.1 Heat Transfer in the pot	11
2.5 Principle of convection.....	15
2.5.1 Natural convection.....	16
2.6 A simple estimate – open heat exchanger parameters.....	17
2.6.1 Results of design and drawings	19
3. MEASUREMENT	20
3.1 Introduction	20
3.2 Measurement components and process	20
3.2.1 Thermocouple	20
3.2.2 Digital unit and Software.....	21
3.3 Analyzing	23
3.4 Installation.....	23
3.5 Results	23
3.5.1 Monitoring of current situation (before plate installation).....	23
3.5.2 Monitoring with installed plate	25
3.6 Errors	31
4. MODELLING	33
4.1 Introduction	33
4.2 Heat transfer theory	33
4.2.1 The energy equation.....	33
4.2.2 Natural Convection and Buoyancy - Driven Flows	34
4.3 Modelling natural convection in a closed domain.....	35
4.3.1 The Boussinesq Model.....	35
4.4 GAMBIT	36
4.5 Results and discussions	37
4.5.1 Modelling of pot according to current situation:	37
4.5.2 Modelling of pot with installed plate	39
4.6 Plate design and optimization	44
4.6.1 User-defined function (UDF).....	44
4.6.2 Optimization	44
5. ECONOMY	50
6. CONCLUSIONS	52
REFERENCES	53
APPENDIX A: The sample of a hot pot	55

APPENDIX B: MATLAB code used to analyze data gathered by LABVIEW	55
APPENDIX C: C program to calculate heat transfer coefficient	56

LIST OF FIGURES

1. A schematic view of the hot pot.....	2
2. Outdoor temperature duration curve for Reykjavik in 1949-1990	6
3. Mass flow change according to temperature of inlet water into pot	10
4. Pot's surfaces construction layouts	12
5. Selected sample pot's plan and details	13
6. Schematic view of plate from below	19
7. Schematic plan of plate	19
8. Sections of plate	19
9. Schematic plan of measured points in the pot and their location.....	20
10. Thermocouple voltage with 0°C reference.....	21
11. Substitution of measured reference Temperature for Ice point reference	21
12. Connecting isothermal junctions.....	21
13. Graphical windows interface ability of Labview	22
14. The arrangement of all units connected for data gathering process	22
15. Stainless steel weight to keep wires at their right place	23
16. Air temperature measurement point.....	23
17. Temperature distribution in the pot including air temperature	24
18. Temperature distribution in the pot in longer period while the lid is closed.....	24
19. Temperature distribution in the pot in longer period while the lid is opened	25
20. Relationship between pipe diameter and heat loss, pressure drop and velocity change.....	26
21. Rubber pipe installation steps using pot drainage pipe	26
22. Plate installation in the pot.....	27
23. a) Rubber pipe connections, b) control valve and digital measurement tool.	27
24. First measurement with the plate	27
25. Pot temperature distribution with plate and 0.1 l/s mass flow rate	28
26. Pot temperature distribution with plate and 0.02 l/s mass flow rate	28
27. Plate logging arrangement	29
28. Temperature distribution in the surface of plate within different mass flow rates.....	29
29. Temperature distribution in the pot with 0.03 l/s mass flow rate.....	30
30. Temperature distribution in the pot with 0.025 l/s mass flow rate.....	30
31. Temperature distribution in the pot with 0.04 l/s mass flow rate.....	30
32. Temperature distribution in the pot with 0.05 l/s mass flow rate.....	30
33. Temperature distribution in the pot with 0.02 l/s mass flow rate.....	30
34. Temperature distribution in the pot with 0.035 l/s and 0.03 l/s mass flow rate	30
35. Temperature distribution in the pot with 0.03 l/s mass flow rate.....	31
36. Due to error in the electronic control unit the water consumption within the 46 hours is shown as 31 m ³	32
37. 3D mesh for whole pot.....	36
38. 2D mesh for plate	36
39. Cross-sectional view of pot, water inlet in the left side	38
40. Cross-sectional view of pot, water vertical to water inlet line	38
41. Temperature distribution in the pot.....	38
42. Temperature distribution in the pot.....	38
43. Temperature distribution in the pot.....	38
44. Temperature distribution of pot in different views	38
45. The cross-sectional view of pot regarding to temperature distribution.....	40
46. Temperature distribution in the pot.....	40
47. Temperature distribution in the pot.....	40
48. Temperature distribution in the pot.....	40
49. Temperature distribution in the pot.....	40

	Page
50. The cross-sectional view of pot regarding to temperature distribution.....	42
51. Temperature distribution in the pot.....	42
52. Temperature distribution in the pot.....	42
53. The cross-sectional view of pot regarding to temperature distribution.....	43
54. Temperature distribution in the pot.....	43
55. Temperature distribution in the pot.....	44
56. Effect of different variables of plate on temperature distribution.....	45
57. Temperature distribution in the plate – type G.....	45
58. The temperature distribution in the outflow of plate.....	46
59. Temperature distribution in upper plate of plate.....	46
60. Temperature distribution in the plate – type F.....	46
61. The temperature distribution in outflow of plate.....	47
62. Temperature distribution in upper plate of plate.....	47
63. Temperature distribution in the plate – type H.....	48
64. Temperature distribution in upper plate of plate.....	48
65. Temperature distribution in upper plate of plate.....	48
66. Temperature distribution in the plate – type I.....	48
67. Temperature distribution in upper plate of plate.....	49
68. Temperature distribution in upper plate of plate.....	49

LIST OF TABLES

1. Previous heat transfer experiments for horizontal surfaces.....	5
2. Parameters for heat loss and energy requirement in the hot pot.....	10
3. Construction material's properties.....	13
4. Total area of selected sample building.....	13
5. Inside film resistance, R_i	14
6. Outside film resistance, R_o	14
7. External walls heat transfer coefficient.....	14
8. Roof's heat transfer coefficient.....	14
9. Floor heat transfer coefficient.....	15
10. Total heat transfer coefficient.....	15
11. Results of calculation from EES.....	18
12. The result of calibration.....	31
13. Heat transfer values in different zones.....	37
14. The average temperature at different zones in Kelvin.....	37
15. The maximum temperature at different parts of pot.....	37
16. Heat transfer values in different zones.....	39
17. The average temperature at different zones in Kelvin.....	39
18. The maximum temperature at different parts of pot.....	39
19. Heat transfer values in different zones.....	41
20. The average temperature at different zones of pot.....	41
21. The maximum temperature at different zones of pot.....	41
22. Heat transfer values in different zones.....	42
23. The average temperature at different zones of pot in Kelvin.....	43
24. The maximum temperature at different parts of pot.....	43
25. Results of modelling for different sizes of plate.....	45
26. Heat transfer values in different zones of plate.....	46
27. Heat transfer values in different zones of plate.....	47
28. Heat transfer values in different zones of plate.....	47
29. Heat transfer values in different zones of plate.....	49
30. Mass flow rates in pot during different periods.....	50
31. Summary of economical comparison of tow systems.....	51

1. INTRODUCTION

1.1 Hot pot

In Iceland there is an abundance of geothermal heat used as a source of district heating in most residential areas. It is quite common for people to have hot spas or geothermally heated Jacuzzis at their house, for recreational purposes. However, even in Iceland there are those that use electrically heated Jacuzzis, and the companies that sell those claim that they are cheaper to operate than the geothermal ones. Although that may not be true, due to the fact that the heat is a much cheaper form of energy than electricity, much energy is wasted in the technology currently used for heating the spas.

Currently there is an obvious waste of heat involved in the mixing of hot water in the geothermal district heating system with cold water, before using it as a heat source in the spa. The motivation of this study is therefore to improve energy efficiency in the use of continuously operated geothermally heated spas, as are common in Icelandic homes. As there is no product currently available on the market that makes it possible to emit hot water from the district heating system directly into the pot, the aim of this study is to develop such a unit, an open heat exchanger that releases much of the heat from water into the pool before it enters the pool.

The district heating system provides water at 80°C, which is mixed with 5°C cold water to decrease the temperature down to 45-50°C, then this mixed water will go into the hot pot to be used. There are several types of hot pots. All of them have similar structure. Main differences between them are the means of supplying energy to the pot and the source of energy consumed. These types will be explained briefly.

The simplest type of pot is relatively cheap. The water supply system consists of pipe lines that bring hot water from district heating system and mix it with cold water through a control valve. In this method the water supply is a continuous process and to keep system at an acceptable range of temperature, it is necessary to control temperature manually. If temperature goes rapidly up, it can be very dangerous for people that enter the hot pot. Some advantages of simple type of hot pot are:

- System is very simple and cheap;
- Maintenance is not costly.

And some disadvantages of simple type of pot can be mentioned as:

- Wasting energy: More waste can happen if flow is too large;
- Medium safety: When children are using, it should be supervised frequently (there is no alarm if temperature goes up).

In an automatic type of pot, cold and hot water are mixed and warm water with specified temperature (usually 37- 40°C) is provided for pot. There are sensors to supply water, when system needs to be heated; these sensors are working with set point that has been fixed in electrical safety unit. Some advantages are:

- Less wasting of energy;
- More safety.

And some disadvantages can be mentioned as:

- More expensive than simple type;
- Complicated installation system;
- Professional needed maintenance.

Figure 1 shows the schematic diagram of a pot. Two main conditions should be taken into account for water circulation system: Standby and operating mode.

In standby mode, the pot is always ready for use. There are different kinds of covers to have minimum value for heat loss of system. System will operate in this situation to keep pot's temperature at the certain temperature, but this operation will have minimum effect on energy consuming. When system is under operation mode, heat loss and energy consuming will increase considerably. Water circulating system in this situation will be an important factor.

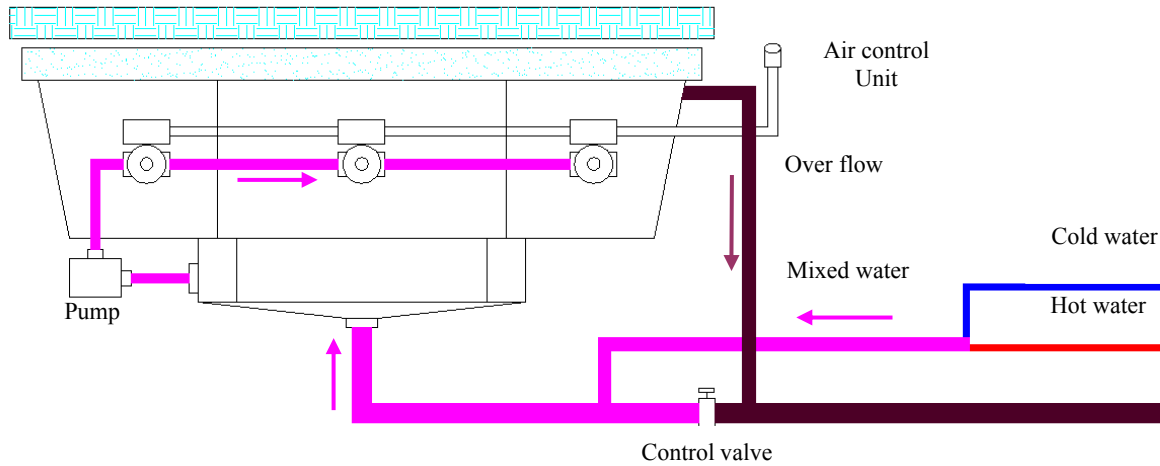


FIGURE 1: A schematic view of the hot pot

Water conveyance, water treatment, and in fact the entire hot pot technology requires pipes and piping system components. The selection of materials plays an important role for the water quality of the entire operation and its service life. According to the maximum flow rate and pressure drop in the water circulation system, circulation pump needs to be selected, also network pressure in district heating system to be used instead of pump.

1.2 Previous work and background

Brief research about the topic has been done with Reykjavik Energy Co. [Orkuveita, 2008]; results show considerable wasted energy from pots. There is not too much literature that specifically pertinent to hot spas and small pools. But it maybe viewed as a swimming pool on a very small scale, publication done on pools and their related fields are considered as a reference sources for the literature studies. The thesis is arranged as follows: In Chapter 2, methodology and steps of heat loss calculation will be described using available references. After all analysis and investigations, an open heat exchanger in the form of a plate is shown to be an acceptable option to feed hot water into pot. It was assumed that convection is the most predominated heat transfer mechanism in the pot.

1.2.1 Free convection from horizontal plates, isothermal surfaces

The average heat-transfer coefficient from horizontal flat plates is calculated with Equation 1.1 and constants given in Table 7-1 in the book by Holman (2001):

$$\overline{Nu}_f = C(Gr_f Pr_f)^m \quad (1.1)$$

The characteristic dimension for use with these relations has traditionally (McAdams, 1954) been taken as the length of a side for a square, the mean of the two dimensions for a rectangular surface, and $0.9d$ for a circular disk. References (Liyod and Moran, 1974, Goldstein et al., 1973) indicate that better agreement with experimental data can be achieved by calculating the characteristic dimension with

$$L = \frac{A}{P} \quad (1.2)$$

where A is the area and P is the perimeter of the surface. This characteristic dimension is also applicable to unsymmetrical planforms.

Natural convective flows over horizontal, heated surfaces appear in a wide variety of industrial equipment as well as in many natural circumstances, they have not been as extensively studied as flows adjacent to vertical surfaces. This is mainly due to the fact that the flows adjacent to horizontal surfaces are complicated and easily become three-dimensional when the plates are of practical sizes. This has hampered analytical treatments. Therefore, in order to obtain basic information on the flow and heat transfer of natural convection, experimental investigations are necessary.

Table 1 shows previous heat transfer experiments carried out with horizontal plates of square or rectangular plan-forms. Isothermal test plates were utilized in most of these experiments. The table summarizes the sizes of the test plates, experimental ranges of Rayleigh numbers which are based on the width of the plates, measured quantities together with the measurement techniques, principal results and other relevant experimental conditions. Among these experiments, the work by Fishenden and Saunders (1957) may be the first that correlated the overall heat transfer coefficients of the horizontal plates with the form:

$$Nu_d = CRa_d^n \quad (1.3)$$

They determined empirically the following sets of coefficients C and exponent n of the equation as: $C = 0.54$, $n = 1/4$ and $C = 0.14$, $n = 1/3$ for the laminar and turbulent flows respectively.

Thereafter, several authors measured the overall heat transfer coefficients of plates with different sizes and planforms using various techniques. Although some authors listed in the table focused their main concerns on inclined plates rather than horizontal plates, they all proposed the coefficients C and the exponents n for horizontal plates. It can be seen the authors have classified the flows into laminar and turbulent flows based on the Rayleigh numbers of the plates. Then, they recommended different sets of coefficients and exponents for each flow. These results are helpful for estimating the overall heat transfer under prescribed surface conditions. However, they give little insight into the flow and temperature fields over the plates. Meanwhile, the visualization study by Husar and Sparrow (Husar and Sparrow, 1968) may be the first work that dealt with the flow field over horizontal heated surfaces. An electrochemical technique was used to visualize the flow field. They observed that the flows move along parallel paths over the plate and reach the central region of the plate.

Rotem and Claassen (1969) carried out the visualization experiments for air using a semifocusing Schlieren apparatus. They reported that laminar boundary layers exist near the plate edges and then break down into irregular convection patterns some distance from the edges.

Pera and Gebhart (1973) measured the temperature distribution and the local heat transfer coefficients of the laminar boundary layer flows of air by using a Mach-Zender interferometer. They revealed that the laminar boundary layers begin to separate when the value of $Gr^{1/3}$ exceeds 80.

Ishiguro et al. (1977) carried out the visualization experiments also by means of a Mach-Zender interferometry. They reported that the temperature fields over the plate become three-dimensional when the Rayleigh numbers based on the plate width exceed 105. Reviewing these experiments on flow and temperature fields over plates, laminar boundary layer flows in the vicinity of leading edges have been the main subject of previous investigations. Contrary to this, very little interest has been directed towards flow and temperature fields in the downstream region of boundary layers, where flow separation and transition to turbulence take place.

Pera and Gebhart (1973) reported by means of smoke tests that the separation occurs three-dimensionally. The transition to turbulence is another subject that has not been fully investigated.

The flow separation and the turbulent transition exert serious influences on the local heat transfer. Although Ishiguro et al. (1977) and Yousef et al. (1982) have measured the local heat transfer coefficients in the downstream region of the separation; their results afford limited information on the correlation between the flow fields and the local heat transfer characteristics.

Natural convective flows over upward-facing horizontal plates were investigated experimentally by Kenzo et al. (Hassani and Hollands, 1987). Extensive measurements of the local heat transfer coefficients were also carried out. The result from the wide plates showed that the following four regions appear over the plates at a streamwise distance x from the leading edge: (1) a laminar boundary layer region, (2) a streaky, transitional flow region, (3) a turbulent region and (4) a collision region. In particular, the second region covers a considerable portion of the total surface, and the local heat transfer coefficients there decrease proportionately with x . Thus, it was found that the width of the plates exerts a serious influence on the average heat transfer coefficients even at the highest Rayleigh numbers of the experiments. Furthermore, empirical correlations for the local and average Nusselt numbers were proposed based on these data.

Al-Arabi and El-Riedy (1976), concluded: 1) Corners have a negligible effect on the average heat transfer from the plate; 2) The average heat transfer coefficient from a circular plate can be considered equal to the average heat transfer coefficient from a square plate with side length equal to diameter of the circular plate.; and 3) The average heat transfer coefficient from a rectangular plate can be considered equal to the average heat transfer coefficient from a square plate with side length equal to the widths of the rectangular plate.

Hassani and Hollands (1987) performed experiments measuring the natural convection heat transfer from a circular disk in both vertical and horizontal configurations, and proposed a characteristic length such that the experimental data obtained could be collapsed with certain other shapes for a limited range of the Rayleigh number.

Pretot et al. (2000) reported a numerical and experimental study of the natural convection flow (of air) above an upward facing horizontal heated plate. The results show the existence of two regions situated near the sides of the plate, which break away in the middle of the heated surface and form a thermal plume. The local heat transfer coefficient is higher near the sides of the plate and decreases at the central heated region.

1.2.2 Forced convection

The essential ingredients of forced convection heat transfer analysis are given by Newton's Law of Cooling:

$$\dot{Q} = hA(T_w - T_\infty) = hA\Delta T \quad (1.4)$$

The rate of heat \dot{Q} transferred to the surrounding fluid is proportional to the object's exposed area A , and the difference between the object temperature T_w and the fluid free-stream temperature T_∞ . The constant of proportionality h is termed the convection heat-transfer coefficient. Other terms describing h include film coefficient and film conductance (Efunda, 2008).

TABLE 1: Previous heat transfer experiments for horizontal surfaces

Reference	Kenzo et al. (1995)	Yousef et al.. (1982)	Ishiguro et al.. (1977)	Al-Arabi and El-Riedy (1976)	Goldstein et al.. (1973)	Fujii and Imura (1972)	Hassan and Mohamed (1970)	Fishenden and Saunders (1957)
Fluid	water	air	water	air	air	water	air	air
Test plate dimensions W*L in cm²	W=2-150 Aspect ratio = 3 Spanmax = 50 cm	10*10 20*20 40*40 (square)	0.76*8 2.8*13 20.5*17	15*(25-60)	W=2.03-5.84 Aspect ratio = 7	5*10 30*15	20*50.4	Max. 60*60 (square)
Collar+/- Fence	Collar+ fence	collar collar collar	collar collar collar +fence	none	none	fence	none	none
Range of Ra numbers	$10^6 < Ra < 10^{15}$	$1.9 * 10^6 < Ra < 1.7 * 10^8$	$3 * 10^5 < Ra < 10^{10}$	$2 * 10^5 < Ra < 10^9$	$2.8 * 10^2 < Ra < 9 * 10^3$	$7 * 10^6 < Ra < 2 * 10^8$ $5 * 10^8 < Ra < 6 * 10^{10}$	$1.1 * 10^2 < Gr < 3 * 10^8$	$10^5 < Ra < 3 * 10^{10}$
Measured quantities (technique)	LHTC (thermocouples) Visualization of flow and temperature field	AHTC LHTC Fluid temp. (Mach-Zender)	AHTC LHTC Visualization	AHTC (amount of condensate)	AMTC (naphthalene sublimation)	AHTC (thermocouples)	AHTC (heat flux meter)	AHTC
Heat transfer correlations	Based on $Nu = C Ra^n$ Sets of coefficient C and exponent n were suggested	Laminar: $3 * 10^6 < Ra < 4 * 10^7$ $Nu = 0.622 Ra^{1/4}$ Turbulent: $4 * 10^7 < Ra < 1.7 * 10^8$ $Nu = 0.162 Ra^{1/3}$	$Nu = 0.2 Ra^{1/3}$	Laminar: $2 * 10^5 < Ra < 4 * 10^7$ $Nu = 0.70 Ra^{1/4}$ Turbulent: $4 * 10^7 < Ra < 10^9$ $Nu = 0.155 Ra^{1/3}$	$Sh = 0.59 Ra^{1/4}$ ($Sc = 2.5$)	$Nu = 0.16 Ra^{1/3}$ $Nu = 0.13 Ra^{1/3}$	$Nu = 0.12 Gr^{1/3}$	Laminar: $10^5 < Ra < 2 * 10^7$ $Nu = 0.54 Ra^{1/4}$ Turbulent: $2 * 10^7 < Ra < 3 * 10^{10}$ $Nu = 0.14 Ra^{1/3}$

AHTC: Average heat transfer coefficient; AMTC: Average mass transfer coefficient;
LHTC: Local heat transfer coefficient; +collar stands for the insulated extension plate upstream of the test plate

2. METHODOLOGY AND DESIGN

2.1 Introduction

According to available references, there are different possible methods to calculate heat demand in the pot. Three scenarios that are covering present and suggested methods of heating the pot will be discussed in this chapter. These scenarios are: 1) Close loop heat exchanger, 2) Manual mixing of cold and hot water, and 3) Open heat exchanger.

The main parameter for district heating system's performance is the weather. The influence of weather on the operation of district heating system is mainly through the outdoor temperature. In this work, the only parameter used to describe weather conditions is outdoor temperature. Measurement data of outdoor temperature for Reykjavik for the years 1949 – 1990 is used for the calculation. The measurements were made at three hours interval. This 42 year weather data shows that the lowest temperature observed in Reykjavik was -17.3°C and the highest is $+24.1^{\circ}\text{C}$. Outdoor temperature was below 15°C for 99.4% of the time, where heating is needed and was above $+19^{\circ}\text{C}$ for only 30 measurements, where heating is not needed.

Outdoor temperature was below -10°C for only 0.57% of the time (Pall Valdimarsson, pers. comm.). From this, one can say that heating is needed for almost all the year around in order to obtain 20°C indoor temperature in the buildings. Outdoor temperature duration curve for Reykjavik, with an inverted temperature scale and normalized time scale is shown in Figure 2. This relatively cool climate along with good sources of geothermal heat makes a sound basis for district heating in urban areas, which has been widely implemented. The district heating system is therefore a reliable heat source to supply heat into pot.

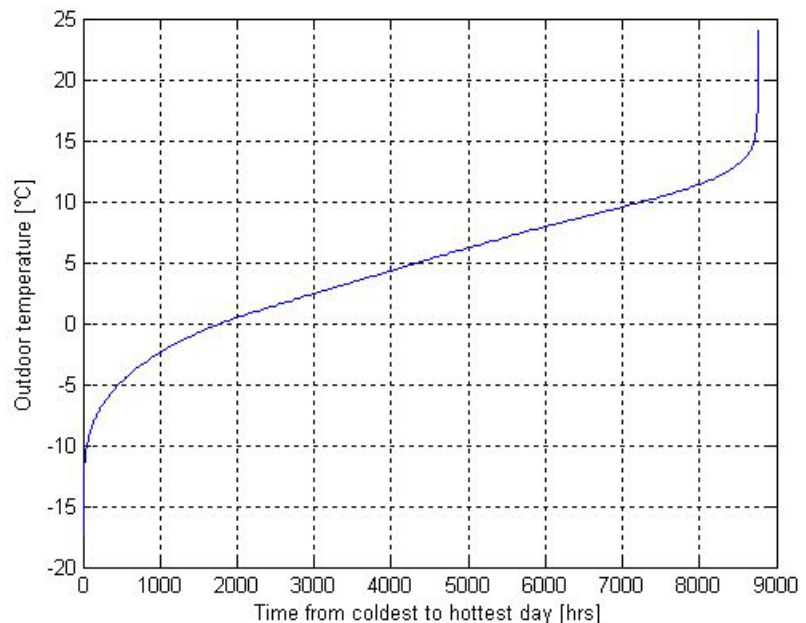


FIGURE 2: Outdoor temperature duration curve for Reykjavik in 1949-1990

2.2 Closed loop heat exchanger

Cold water will pass through the heat exchanger to be heated by geothermal water. The system is closed and make up water tank and strong filtering system is required. Calculation for this section is according to general design method for pools (Svavarsson, 1990). Sizes of pot are different; costumers can order according to members of family, it is normally designing from 3 to 5 people. Also many different shapes are available. It comes to market in very simple circular shape up to very complicated rectangular shapes. The pot which is used as a case in this study is shown on a drawing in Appendix A (Normx, 2007). Selected pot has two steps. Main step's depth will be 0.5 m, and depth for second step will be 0.2 m. Dimensions are shown in Appendix A. According to these values, the total water volume of the hot pot will be 2 m^3 . Figure 1, shows the schematic diagram of pot, two main conditions should be taken into account for water circulation system, as follows:

- Standby: most families like to have hot pot ready, for any time that they like. For this reason there are different kinds of covers to have minimum value for heat loss of system.

System will operate in this situation to keep pot's temperature at the certain temperature, but this operation will have minimum effect on energy consuming.

- Operating: when system under operation, heat loss and energy consuming will increase considerably. Water circulating system in this situation will be important factor. This project will discuss this condition further.

The turnover period is one of the most important factors in operation of the pools. It is the time it takes to circulate the whole of the water in the pot through the all outlets and inlets and all circulation lanes. It changes with the pot loading and mostly depends on the type of pot. The turnover period has been calculated equal to 9.5 hours (Perkin, 1988). Fat, hair and other impurities can be controlled with complicated system, includes chlorine, coagulation and filtering units. They are costly and mostly are using in public pools. For Hot pot there are flout units that are doing sanitary cares as well as these complicated expensive unites.

2.2.1 Heat loss from pot

Heat loss from outdoor pools is mainly due to (Svavarsson, 1990):

- Convection
- Evaporation
- Radiation
- Conduction
- Rain

The main heat loss mechanisms from the pot are convection and evaporation. The obtained results from earlier researches and analyses show that heat losses due to the other three factors (radiation, conduction, rain) can be estimated to be equal to 10% of total heat loss due to convection and evaporation. Heat loss due to conduction is small, because of good insulation in the pot building materials; also the heat loss contribution due to rain and radiation is not very big so in the following calculation 10% of total heat loss by convection and evaporation will be assumed for these three mentioned factors.

Heat loss due to convection. Heat loss due to convection depends strongly on the air temperature around the pot and the wind speed. Equation 2.1 shows that heat loss through convection will increase with higher wind speed and lower outside temperature:

$$q_C = h_c(T_w - T_a) \quad (2.1)$$

where q_c = Amount of heat loss by convection (W/m^2);
 T_w = water temperature in the pot ($^{\circ}C$);
 T_a = Air temperature in the pot's around ($^{\circ}C$);
 h_c = Convection heat transfer coefficient ($W/m^2^{\circ}C$), it is very dependent on wind speed.

The relationship between heat transfer coefficient and wind speed is shown in Equation 2.2, which is named Rimsha-Doncenko formula:

$$h_c = 4.19(k + 0.45v) \quad (2.2)$$

where v = Wind speed at 2 meter height from the ground surface (m/s);
 k = Empirical coefficient ($W/m^2^{\circ}C$) as shown in Equation 2.3.

$$k = 0.93 + 0.04(T_w - T_a) \quad (2.3)$$

Heat loss due to evaporation. Heat loss due to evaporation takes place when there is different partial pressure of water vapor at the pot's surface and in the air over the pool. This will cause evaporation of water at the pot surface and this requires energy which is taken from the water. This kind of heat loss in the pot can be calculated with Equation 2.4 obtained from Rimsha – Doncenko (Svavarsson, 1990):

$$q_E = (1.56k + 0.70v^2).(e_W - e_a) \quad (2.4)$$

where q_E = Amount of heat loss by evaporation (W/m^2);
 e_W = Partial pressure of steam at surface (mbar);
 e_a = Partial pressure of steam in the air over pot (mbar).

According to these results and explanation about heat loss due to radiation, conduction, rain Equation 2.5 can be written:

$$q_T = q_E + q_C + S \quad (2.5)$$

where q_T = Total heat loss from the pot (W/m^2);
 S = 10%($q_E + q_C$) (W/m^2).

Both input and calculated parameters are shown in Table 2. The total heat loss from the pot is 11.3 kW.

Energy requirement for heating the pot. The total heat loss from hot pot has been calculated and the same quantity of heat must be added to the water supplied to the pot. This is done through a heat exchanger that, transfers heat from district heating water to fresh water which is used as pot water. According to the above explanation, Equation 2.6 can be written:

$$q_T = q_i \quad (2.6)$$

where q_i = Required quantity of heat for the pot (W/m^2).

Equation 2.7 (Wark, 1988), is used for calculation of the amount of geothermal water needed as a heat source and amount of required water for circulation in the system according to desired temperature for supply water. The results are 0.09 kg/s and 0.21 kg/s respectively with supply temperature equal to 50°C. Equation 2.7 is known as the energy balance equation in the steady-flow condition:

$$Q_i = m_1 C_{p1} (T_2 - T_1) = m_2 C_{p2} (T_3 - T_4) \quad (2.7)$$

where m_1 = Amount of water required for circulated in the system (kg/s);
 m_2 = Amount of geothermal water as a heat source (kg/s);
 C_p = Specific heat capacity of water ($J/kg^\circ C$);
 T_1 = Temperature of pot's cold water before heated by heat exchanger ($^\circ C$);
 T_2 = Temperature of pot's heated water by heat exchanger ($^\circ C$);
 T_3 = Temperature of inlet geothermal water at heat exchanger ($^\circ C$);
 T_4 = Temperature of outlet geothermal water at heat exchanger ($^\circ C$);
 Q_i = Amount of required heat for the pot (W).

The piping system of the hot pot. Water conveyance, water treatment, and in fact the entire hot pot technology requires pipes and piping system components. The selection of materials plays an important role for the water quality of the entire operation and its service life. Thermal water has curative properties, but is also aggressive and may cause corrosion; all pipes made of polypropylene (PP) or polyethylene (PVC) have passed the tests, so the pipe material chosen is PVC and PP which can resist the above conditions (Normx, 2007). The water distribution system in the hot pot will be accomplished with the piping system. The turnover period is the main factor for determining the piping system properties and the amount of mass flow through the pipes in the walls of the pot. Calculation of turnover time is shown below.

According to size of hot pot as mentioned in introduction, the water volume will be 2 m³:

$$V_{pot} = 2m^3 \quad (2.8)$$

where V = Water volume (m^3).

According to Equation 2.7, the desired supply temperature, and calculated heat loss and mass flow, turnover time can be calculated:

$$T_o = \frac{V}{m} = \frac{2}{0.21} = 9.53 \text{ hours} \quad (2.9)$$

where m = Mass flow rate (l/s);
 T_o = Turnover period (hour).

The number of inlet nozzles in the floor and wall of the pot can differ, mostly with the size of the pot and the complexity of the feeding system. In most cases 1 to 4 inlet nozzles are located on the walls. Also one extra or in some cases main feed nozzle is located in the floor of the pot. In the pot studied in this work there is only one inlet nozzle located at the bottom side wall. According to number of inlet nozzles the mass flow through each of them can be calculated:

$$m_{in} = \frac{m}{n_o} \text{ l/s / Inlet nozzle} \quad (2.10)$$

where m_{in} = Mass flow rate per inlet nozzle (l/s);
 n_o = Number of inlet nozzle in the bottom of the pool.

Pressure drop calculation and pump selection. According to the maximum flow rate and pressure drop in the water circulation system, circulation pump is selected. Maximum flow rate has been calculated to be 0.21 l/s. One way of calculating the pressure drop in the pipelines is using Equation 2.11 (Olson, 1973), assuming an appropriate value for the roughness factor (k).

$$\Delta P = \frac{\rho v^2}{2} \cdot \frac{fL}{D} \quad (2.11)$$

where ΔP = Pressure drop (kPa);
 f = $1 / (2 \log(D/2k + 1.74))^2$;
 K = Roughness factor;
 ρ = Density of fluid (kg/m^3);
 v = Velocity of fluid (m/s);
 L and D = Length and diameter of pipe respectively (m).

Evaluation criteria and boundary conditions. The three most important criteria are strict safety conditions for users with minimum possible cost and instruments with long service life. A comfortable temperature of water inside of hot pot is around 40°C. The maximum possible temperature allowed for water inside the hot pot is 50°C. Higher temperatures are potentially dangerous for users. This is therefore used as a boundary condition.

Table 2 shows all input and calculated parameters in the calculation of the required heat for the pot, the geothermal water's flow rate, pot water temperature after heat exchanger and the total heat loss from the pot.

TABLE 2: Parameters for heat loss and energy requirement in the hot pot

Known factors (design condition)	Factors	Value	Unit
Air temperature	T_a	-5	$^{\circ}\text{C}$
Wind speed	v	8	m/s
Humidity (max)	H	60	%
Amount of required water for circulated in the system	m_1	0.21	l/s
Amount of required water for circulated in the system	m_1	0.21	kg/s
Specific heat capacity of water	C_{p1}	4.18	$\text{kJ/kg}^{\circ}\text{C}$
Temperature of pot's cold water before heated by heat exchanger	T_1	37	$^{\circ}\text{C}$
Specific heat capacity of water	C_{p2}	4.18	$\text{kJ/kg}^{\circ}\text{C}$
Temperature of inlet geothermal water at heat exchanger	T_3	75	$^{\circ}\text{C}$
Temperature of outlet geothermal water at heat exchanger	T_4	45	$^{\circ}\text{C}$
Area of pot	A	4	m^2
Calculated values	Factors	Value	Unit
Amount of required heat for the pot	Q_i	11.3	kW
Amount of geothermal water as a heat source	m_2	0.09	kg/s
Temperature of pot's heated water by heat exchanger	T_2	50	$^{\circ}\text{C}$
Coefficient depends on temperature difference	K	11.4	$\text{W/m}^2^{\circ}\text{C}$
Heat transfer coefficient	h_c	26.5	$\text{W/m}^2^{\circ}\text{C}$
Convictional heat loss	Q_C	1193	W/m^2
Partial pressure of steam at water surface	e_w	35.7	mbar
Partial pressure of steam in the air over pot	e_a	2.41	mbar
Amount of heat loss by evaporation	Q_E	1374	W/m^2
Total heat loss from the pot	Q_T	2823	W/m^2

2.3 Manual mixing of cold and hot water

Mixture of cold and hot water with 45°C will be fed into pot to maintain the temperature of pot at 40°C .

2.4 Open heat exchanger

Water at 75°C is fed into an open heat exchanger through which it dispels heat to the surrounding water in the pot and is cooled to 50°C before it mixes with the water in the pot. The water entering the heat exchanger therefore renews the water in the pot.

Scenarios 2.3 and 2.4 are very similar due to calculation process; just the inlet water temperature is different. According to Figure 3, 0.012 kg/s of water at 75°C is needed to maintain the desired temperature in the pot. The mass flow is 0.043 kg/s while the water temperature is 50°C . This is actually the present situation for pots that mixes hot and cold water to pump the 50°C water into pot.

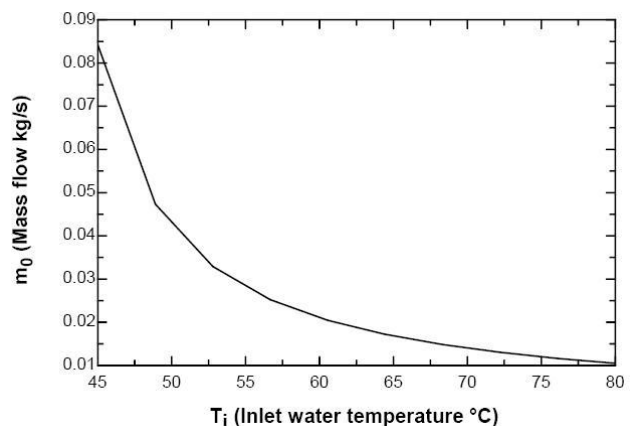


FIGURE 3: Mass flow change according to temperature of inlet water into pot

2.4.1 Heat transfer in the pot

In order to calculate heat load in the pot, relationship between pot and its surroundings must be defined. Heat transfer is a transient flow of thermal energy from one system to another due to temperature difference between two systems. There are three kinds of heat transfer: conduction, convection and radiation. In most cases heat transfer is dominated by conduction and convection.

Heat transfer calculation. When systems are static and in physical contact, heat transfer will be happen with conduction. This transient will be from the hotter molecule to the cooler molecule. Heat transfer rate per unit area is proportional to the normal temperature gradient. Thus;

$$\frac{q_c}{A} \sim \frac{\Delta T}{\Delta x} \quad (2.12)$$

Fourier's law for one dimension:

$$q_c = -kA \frac{dT}{dx} \quad (2.13)$$

Equation 2.13 can be simplified by assuming that heat transfer in the homogeneous, k is constant, so the following equation is concluded:

$$\frac{q_c}{A} = \frac{k}{\Delta x} (T_1 - T_2) \quad (2.14)$$

where Δx is the thickness separating the surfaces, which are at T_1 and T_2 .

By rearranging equation 2.14, the following relation is obtained:

$$\frac{q_c}{A} = \frac{(T_1 - T_2)}{\Delta x / k} = \frac{T_1 - T_2}{R_c} \quad (2.15)$$

where R_c is the thermal resistance due to conduction, which is defined as follows:

$$R_c = \Delta x / k \text{ (m}^2\text{C/W)} \quad (2.16)$$

For one composite components (wall, floor, roof, etc) made of different layers and number of materials (Figure 4), the following relationship can be obtained, with regard that heat flow is the same in each of the layers, thus.

$$q_c = q_{c1} = q_{c2} = q_{c3} \quad (2.17)$$

$$q_c = \frac{T_1 - T_2}{\Delta x_1 / k_1 A} = \frac{T_2 - T_3}{\Delta x_2 / k_2 A} = \frac{T_3 - T_4}{\Delta x_3 / k_3 A} \quad (2.18)$$

By solving Equation 2.18, it can be concluded that:

$$\frac{q_c}{A} = \frac{T_1 - T_4}{\Delta x_1 / k_1 + \Delta x_2 / k_2 + \Delta x_3 / k_3} \quad (2.19)$$

or

$$\frac{q_c}{A} = \frac{T_1 - T_4}{R_1 + R_2 + R_3} \quad (2.20)$$

$$\frac{q_c}{A} = \frac{T_i - T_o}{R_o + R_1 + R_2 + R_3 + R_i} \quad (2.21)$$

where R_o and R_i are the outside and inside film thermal resistances of the fluid respectively.

Therefore, the total thermal resistance of heat transfer is given as follows:

$$R = R_o + \sum_{k=1}^n R_k + R_i \quad (2.22)$$

where, n is the total number of layers of the composite wall.

The overall heat transfer coefficient of the wall is defined as follows:

$$U = \frac{1}{R} \quad (2.23)$$

Therefore, the heat transfer from the building to the environment can be calculated according to the following formula:

$$q_c = UA(T_i - T_o) \quad (2.24)$$

where T_i and T_o are the inside and outside design temperature respectively.

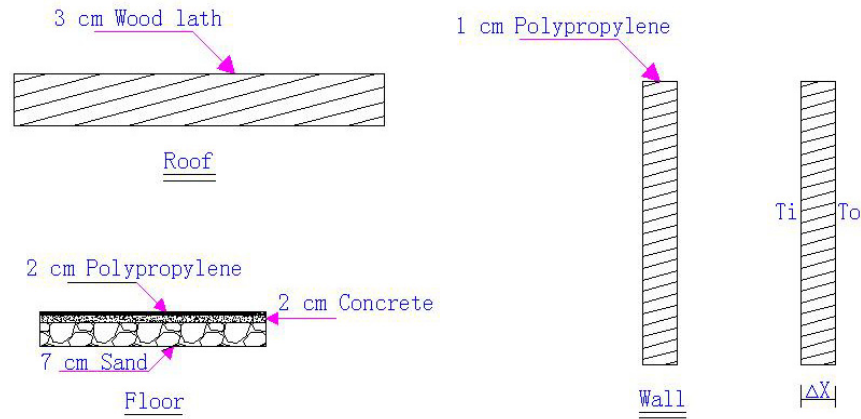


FIGURE 4: Pot's surfaces construction layouts

Convection heat transfer. When, heat is transferred between two systems by means of a moving fluid such as air or water, we have heat transfer by convection. There are two types forced convection and free convection. Newton's law of cooling in the following equation is the general equation for heat transfer by convection:

$$q_h = h.A(T_w - T_o) \quad (2.25)$$

where h = Convection heat transfer coefficient ($W/m^2\text{°C}$), value of this parameter depends on the complexity of the system;
 A = Heat transfer surface area (m^2);
 T_w = Wall surface temperature (°C);
 T_o = Air temperature (°C).

Equation 2.25 also can be rearranged as follows:

$$q_h = \frac{T_w - T_o}{1/hA} = \frac{T_w - T_o}{R_{conv}} \quad (2.26)$$

where, $R_{conv} = 1/hA$ which is thermal resistance due to convection heat transfer.

Radiation heat transfer. Heat transfer by conduction and convection require a medium for existence, this activity by radiation can take place in vacuum, and it is an electromagnetic radiation. The net heat exchange by radiation between two objects is given by the following equation:

$$q_r = \sigma A_1 F_{1-2} \varepsilon (T_1^4 - T_2^4) \quad (2.27)$$

where q_T = Rate of heat transfer by radiation (W);
 σ = Stefan-Boltzman constant ($5.669 \times 10^{-8} \text{ W/m}^2 \cdot \text{K}^4$);
 A_1, A_2 = Area of surface 1 and surface 2 (m^2);
 F_{1-2} = This factor indicates the fraction of energy between two objects;
 ε = Common emissivity of the objects;
 T_1, T_2 = The temperature of surface 1 and surface 2, respectively ($^{\circ}\text{C}$).

Main body of the pot. Figure 5 is a drawing showing the dimensions of the pot used in the case study. The pot is outdoors and is fitted with a lid that closes the pot and keeps the surface isolated. For calculation a reference outdoor temperature is 0°C and desired pot temperature is 37°C .

Construction materials. For calculation, construction material's properties must be defined (M. Fishenden et al., 1957); the body of pot is divided into walls, roof and floor, Table 3 shows the construction of mentioned surfaces, while Table 4 shows the total area of roof, floor, walls and windows of sample building.

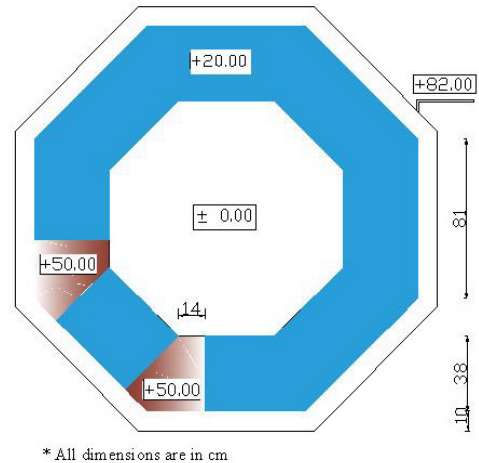


FIGURE 5: Selected sample pot's plan and details

TABLE 3: Construction material's properties

Construction material	Density (kg/m^3)	Thermal conductivity λ ($\text{W/m}^{\circ}\text{C}$)	Heat capacity ($\text{kJ/kg}^{\circ}\text{C}$)
Wood lath	640	0.15	2.8
Polypropylene	1150	0.16	1.90

TABLE 4: Total area of selected sample building

Area type	Area (m^2)
Roof	3.2
Floor	3.2
Walls	4.54

Heat transfer coefficient. Heat transfer coefficient is a constant describing the heat transfer between a structure and its environment due to conduction, convection and radiation heat loss, the calculation according to the following formula:

$$U_{total} = \frac{U_1 A_1 + U_2 A_2 + \dots}{A_{total}} \quad (2.28)$$

where U_n = Heat transfer coefficient of different components constituting building surroundings (walls, windows, ceilings and floors), ($W/^\circ C m^2$);
 A_n = Each component surface area, (m^2);
 A_{total} = Total surface area of the building, (m^2).

The heat transfer coefficient is calculated under no insulation condition.

Walls heat transfer coefficient. The walls film resistance and total heat transfer coefficient is given in Tables 5-7.

TABLE 5: Inside film resistance, R_i

Element	Heat direction	Material type	R_i ($m^2^\circ C/W$)
Walls	Horizontal	Construction materials	0.12
Ceilings and floors	Upward	Construction materials	0.10
	Downward	Construction materials	0.15

TABLE 6: Outside film resistance, R_o

Wind speed (m/s)		≤ 0.5	0.5-5.0	≥ 5.0
Element	Material type	R_o ($m^2^\circ C/W$)		
Walls	Construction materials	0.08	0.06	0.03
Ceilings and floors	Construction materials	0.07	0.04	0.02
Exposed Floors	Construction materials	0.09	-	-

TABLE 7: External walls heat transfer coefficient

Construction material	X (m)	K ($W/m^\circ C$)	R ($m^\circ C/W$)
Polypropylene	0.01	0.16	0.06
R_i			0.12
R_o			0.03
R_{total}			0.21

$$U_{wall} = 1/0.213 = 4.71 (W / m^2^\circ C)$$

Roof heat transfer coefficient is given in Table 8.

TABLE 8: Roof's heat transfer coefficient

Construction material	X (m)	K ($W/m^\circ C$)	R ($m^\circ C/W$)
Wood lath	0.03	0.15	0.20
R_i			0.10
R_o			0.02
R_{total}			0.32

$$U_{roof} = 1/0.32 = 3.13 (W/m^2^\circ C)$$

Floor heat transfer coefficient. The floor's total heat transfer coefficient is given in Table 9.

TABLE 9: Floor heat transfer coefficient

Construction material	X (m)	K (W/m°C)	R (m°C/W)
Sand	0.07	0.38	0.18
Concrete	0.02	1.4	0.01
Polypropylene	0.01	0.16	0.06
Ri			0.15
Ro			0.09
R_{total}			0.50

$$U_{floor} = 1/0.501 = 2 \text{ (W/m}^2\text{°C)}$$

Pot total heat transfer coefficient. After determining each surroundings heat transfer coefficient, the total pot's heat transfer coefficient can be easily determined using Equation 2.28, it is shown in the Table 10.

TABLE 10: Total heat transfer coefficient

Surface	U (W/m ² °C)	A (m ²)	UA (W/°C)
Roof	3.13	3.22	10.1
Floor	2	3.2	6.4
External walls	4.71	4.54	21.38
Total		10.96	37.88

$$U_{total} = 37.88/10.96 = 3.46 \text{ (W/m}^2\text{°C)},$$

According to Equation 2.24:

$$q_c = UA(T_i - T_o) = 3.46 * 10.96(40 - 0) = 1516.9W$$

2.5 Principle of convection

The subject of convection heat transfer requires an energy balance along with an analysis of the fluid dynamics of the problems concerned. Heat energy transfers between a solid and a fluid when there is a temperature differences. This is known as "convection heat transfer". Generally, convection heat transfer cannot be ignored when there is a significant fluid motion around the solid. In heat transfer problems, the Prandtl number (Pr) controls the relative thickness of the momentum and thermal boundary layers. When Pr is small, it means that the heat diffuses very quickly compared to the velocity (momentum). This means that for liquid metals the thickness of the thermal boundary layer is much bigger than the velocity boundary layer.

$$Nu_x = \frac{h_x x}{k} \quad (2.29)$$

Nu is called Nusselt number after Wilhelm Nusselt, who made significant contribution to the theory of heat transfer by convection.

$$Nu_x = 0.332 Pr^{1/3} Re_x^{1/2} \quad (2.30)$$

The fluid properties were assumed constant throughout the flow. When there is an appreciable variation between wall and free-stream conditions, it is recommended that the properties be evaluated at the so-called film temperature T_f , defined as the arithmetic mean between the wall and free-stream temperature:

$$T_f = \frac{T_w + T_\infty}{2} \quad (2.31)$$

2.5.1 Natural convection

Fluids receive heat and carry energy in the form of enthalpy as they flow. Heat transfer that results from fluid motion is called convection. The movement of the fluid in free convection, whether it is a gas or a liquid, results from the buoyancy forces imposed on the fluid when its density in the proximity of the heat-transfer surface is decreased as a result of the heating process. The buoyancy forces would not be present if the fluid were not acted upon by some external force field such as gravity, although gravity is not the only type of force field that can produce the free-convection currents; a fluid enclosed in a rotating machine is acted upon by a centrifugal force field, and thus could experience free-convection currents if one or more of the surfaces in contact with the fluid were heated. The buoyancy forces that give rise to the free-convection currents are called body forces.

The heat transfer coefficient. Over the years it has been found that average free-convection heat-transfer coefficients can be found regarding to Nusselt number which is represented in the following functional form a variety of circumstances:

$$\overline{Nu}_f = C(Gr_f Pr_f)^m \quad (2.32)$$

where the subscript f indicates that the properties in the dimensionless groups are evaluated at the film temperature. The product of the Grashof and Prandtl numbers is called the Rayleigh number:

$$Ra = Gr Pr \quad (2.33)$$

The Grashof number may be interpreted physically as a dimensionless group representing the ratio of the buoyancy forces to the viscous forces in the free-convection flow system. It has a role similar to that played by the Reynolds number in forced-convection systems and is the primary variable used as a criterion for transition from laminar to turbulent boundary layer flow. Values ranging between 10^8 and 10^9 may be observed for different fluids and environment “turbulence levels” (Holman, 2001).

According to Table A-9 in Holman (2001) on properties of water:

$$Gr_x Pr = \left(\frac{g\beta\rho^2 C_p}{\mu k} \right) x^3 \Delta T Pr \quad (2.34)$$

where β = Temperature coefficient of thermal conductivity, $1/k$;
 C_p = Specific heat at constant pressure, $\text{kJ/kg } (^\circ\text{C})$;
 k = Thermal conductivity ($\text{W/m}^\circ\text{C}$).

$$Nu_x = C(Gr_x Pr)^m \quad (2.35)$$

Constant heat flux. The experiment of Fujii et al. (1972) has produced the following correlations for constant heat flux on a horizontal plate. For the heated surface facing upward:

$$\overline{Nu}_L = 0.13(Gr_L Pr)^{1/3} \quad \text{for} \quad Gr_L Pr < 2 * 10^8 \quad (2.36)$$

and

$$\overline{Nu}_L = 0.16(Gr_L Pr)^{1/3} \quad \text{for} \quad 2 * 10^8 < Gr_L P < 10^{11} \quad (2.37)$$

$$\overline{Nu}_L = \frac{\overline{h}L}{k} \quad (2.38)$$

where \overline{Nu}_L = Average nusselt number;
 \overline{h} = Average heat transfer coefficient.

2.6 A simple estimate – open heat exchanger parameters

The following analysis was used to determine the design parameters for the open heat exchanger prototype. Temperature under the centre plate is described by the following differential equation (Palson, pers. comm.):

$$cm \frac{dT}{dr} + 2\pi rh(T - T_a) = 0 \quad (2.39)$$

where c is specific heat of water, \dot{m} is the mass flow, T_a is the plate temperature and h is the convection coefficient.

The equation can be solved if the boundary condition $T(0)=T_i$ is given, which is the inflow temperature. It is assumed that the flow is laminar, according to this, the flow velocity as a function of r can be calculated:

$$v = \frac{\dot{m}}{2\pi y \rho} \quad (2.40)$$

where ρ is the water density and y is the gap between plate and pot bottom.

$$R_e = \frac{\rho vr}{\mu} = \frac{\dot{m}}{2\pi y \mu} \quad (2.41)$$

$$N_u = 0.332 * R_e^{1/2} P_r^{1/3} \quad (2.42)$$

$$h = \frac{kN_u}{r} \quad (2.43)$$

Equation 2.39 becomes:

$$cm \frac{dT}{dr} + 2\pi k N_u (T - T_a) = 0 \quad (2.44)$$

then

$$\theta = \frac{T - T_a}{T_i - T_a} \quad (2.45)$$

$$\eta = \frac{r}{R} \quad (2.46)$$

where R is the plate radius.

A dimensionless form of the equation:

$$\frac{d\theta}{d\eta} + \alpha\theta = 0 \quad (2.47)$$

with

$$\alpha = \frac{2\pi k N_u R}{c\dot{m}} \quad (2.48)$$

and the boundary condition $\theta(0) = 1$.

The solution to Equation 2.47 is

$$\theta(\eta) = \exp(-\alpha\eta) \quad (2.49)$$

which can be used to calculate the exit temperature of the water, $\theta(1)$, which then becomes:

$$T_e = T_a + (T_i - T_a) \exp\left(-\frac{2\pi k N_u R}{c\dot{m}}\right) \quad (2.50)$$

The heat flow into the plate is equal to the heat flow from the plate top to the water in the pot. Thus:

$$c\dot{m}(T_i - T_e) = h_i \pi R^2 (T_a - T_p) \quad (2.51)$$

where h_i is the free convection coefficient at the plate top and T_p is the water temperature in the pot.

Furthermore, the heat balance of the pot itself can be formulated as:

$$c\dot{m}(T_i - T_p) = UA(T_p - T_\infty) \quad (2.52)$$

where it is assumed that the water flowing out of the pot has temperature T_p . Here, A is the pot area, U is the heat transfer coefficient between pot and surroundings and T_∞ is the temperature of the surroundings. In order to solve the problem, it is assumed that all parameters are known except \dot{m} , which can be found directly from Equation 2.52, T_e and T_a . After \dot{m} has been found Equations 2.50 and 2.51 can be used to obtain T_e and T_a . It looks important to remind that h_i is generally a function of T_a and T_p . Table 11 illustrates some results from EES calculation, and according to method was described.

TABLE 11: Results of calculation from EES

Parameter	Factors	Value	Unit
Inflow water temp.	T_i	75	$^{\circ}\text{C}$
Pot total heat transfer coefficient	U	3.5	$\text{kW}/\text{m}^2\text{C}$
Air temp.	T_s	0	$^{\circ}\text{C}$
Mass flow rate	m_0	0.012	Kg/s
free convection coefficient	h_t	546.1	$\text{W}/\text{m}^2\text{C}$
Rayleigh no.	Ra	$8.776*10^7$	
Reynolds no.	Re	2153	
Heat loss from pot	q	1.63	kW/m^2
Plate edge temp.	T_e	43.43	$^{\circ}\text{C}$
Plate temp.	T_a	43.43	$^{\circ}\text{C}$
Gap between plates	Y	0.002	m
Radius of plate	R	0.15	m

2.6.1 Results of design and drawings

Next step was to decide for dimensions of plate. It is very important to have feasible size for plate due to possibility of production in future and low cost and easy to use.

According to data from modelling and similar experiences also regarding to available domestic market to make sample product, it was decided to have simple product. The size of 30 cm circular plate was decided to be built and used for testing. Figures 6-8 shows the details of the designed plate.

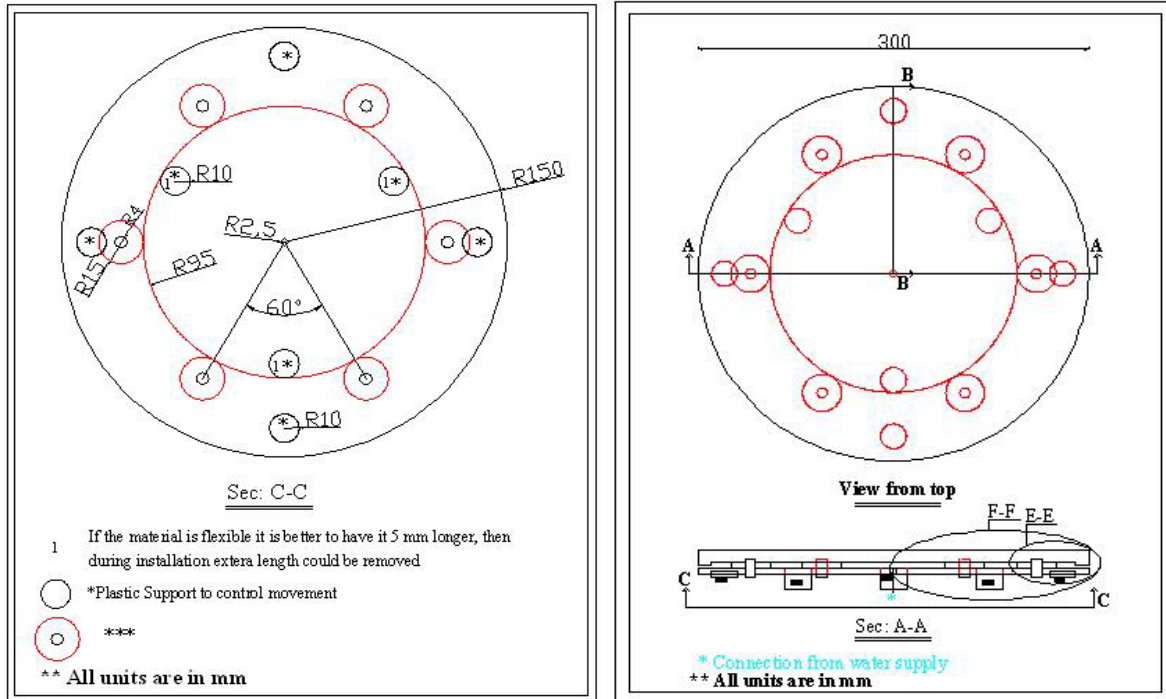


FIGURE 6: View of plate from below

FIGURE 7: Schematic plan of plate

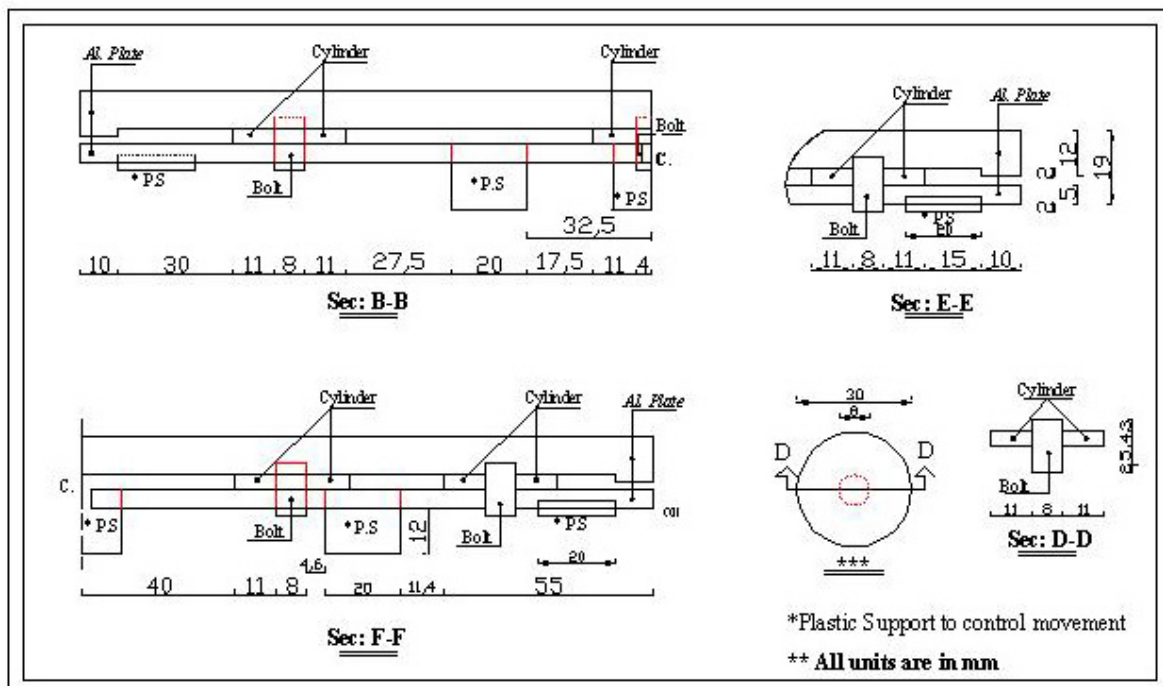


FIGURE 8: Sections of plate

3. MEASUREMENTS

3.1 Introduction

The idea of measurement was to analyze temperature distribution in different points of pot. The explained sample pot was selected to monitor temperature distribution in the pot. Thermocouple amplifiers were used to measure temperature and analogue to digital convertor was used to transfer analogue data to digital. Measurement system was installed in one family house to monitor eight points in different parts of pot as well as air temperature.

The family house is villa home in Gardabaer, Reykjavik, Iceland. Couple is living there and using hot pot daily. The described pot in previous chapters was used to install measurement's tool. Figure 9 shows the arrangement of measured points. The points selected to check temperature profile and to confirm the symmetric situation in the system. As it can be seen from Figure 9, it seems to be enough to measure quarter of pot because of symmetry, but a central line which monitors data from several points was selected.

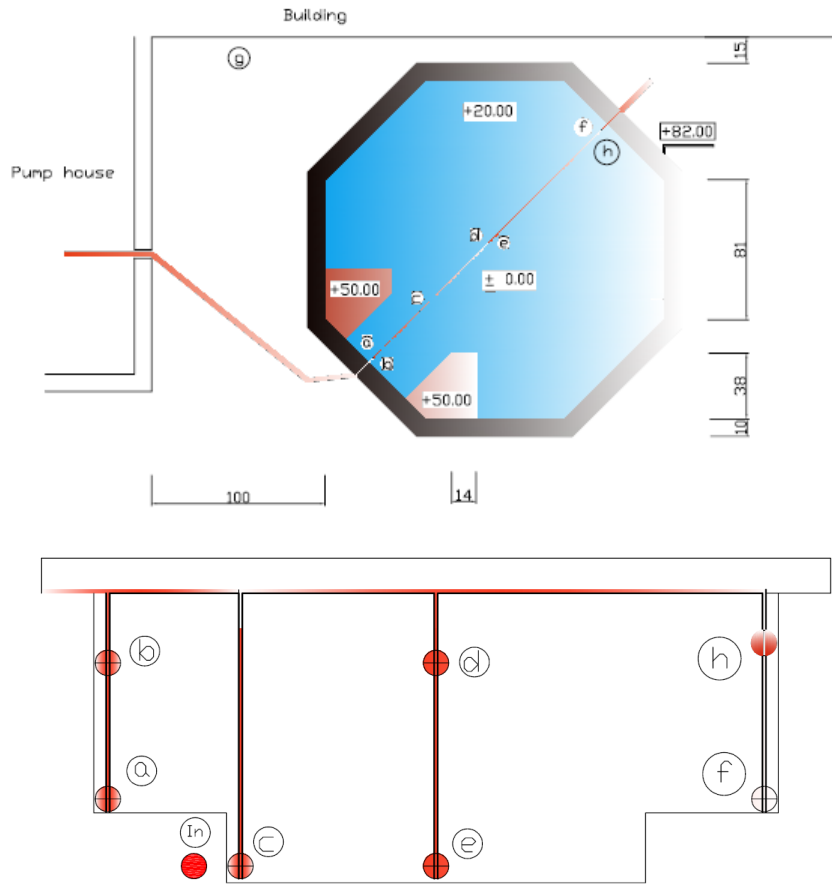


FIGURE 9: Schematic plan of measured points in the pot and their location

3.2 Measurement components and process

3.2.1 Thermocouple

Around 50 m thermocouple wires were used to record data. Thermocouples are economical and rugged; they have reasonably good long-term stability. Because of their small size, they respond quickly and are good choices where fast response is important. They function over temperature ranges from cryogenics to jet-engine exhaust and have reasonable linearity and accuracy.

Because the number of free electrons in a piece of metal depends on both temperature and composition of the metal, two pieces of dissimilar metal in isothermal and contact will exhibit a potential difference that is a repeatable function of temperature, as shown in Figure 10. The resulting voltage depends on the temperatures, T1 and T2, in a repeatable way (Analog Devices, 2007).

Since the thermocouple is basically a differential rather than absolute measuring device, a known reference temperature is required for one of the junctions if the temperature of the other is to be inferred from the output voltage. Thermocouples made of specially selected materials have been

exhaustively characterized in terms of voltage versus temperature compared to primary temperature standards. Most notably the water-ice point of 0°C is used for tables of standard thermocouple performance.

An alternative measurement technique, illustrated in Figure 11, is used in most practical applications where accuracy requirements do not warrant maintenance of primary standards. The reference junction temperature is allowed to change with the environment of the measurement system, but it is carefully measured by some type of absolute thermometer. A measurement of the thermocouple voltage combined with knowledge of the reference temperature can be used to calculate the measurement junction temperature. Usual practice, however, is to use a convenient thermoelectric method to measure the reference temperature and to arrange its output voltage so that it corresponds to a thermocouple referred to 0°C. This voltage is simply added to the thermocouple voltage and the sum then corresponds to the standard voltage tabulated for an ice-point referenced thermocouple.

The temperature sensitivity of silicon integrated circuit transistors is quite predictable and repeatable. This sensitivity is exploited in the AD594/AD595 to produce a temperature related voltage to compensate the reference of “cold” junction of a thermocouple as shown in Figure 12.

Since the compensation is at the reference junction temperature, it is often convenient to form the reference junction by connecting directly to the circuit wiring. So long as these connections and the compensation are at the same temperature no error will result.

3.2.2 Digital unit and software

A Pc with windows operator was used to record data. LabVIEW (Laboratory Virtual Instrumentation Engineering Workbench) was used for data acquisition. Its graphical ability to make simple model of measured points was very helpful. Also it has high capacity to restore data in the format of text file. Figure 13 shows the graphical windows interface ability of software.

Data acquisition (DAQ or DAS), begins with the physical phenomenon or physical property of an object (under investigation) to be measured (Wikipedia, 2007). This physical property or phenomenon could be the temperature or temperature change of a room, the intensity or intensity change of a light source, the pressure inside a chamber, the force applied to an object, or many other things. An effective data acquisition system can measure all of these different properties or phenomena. A

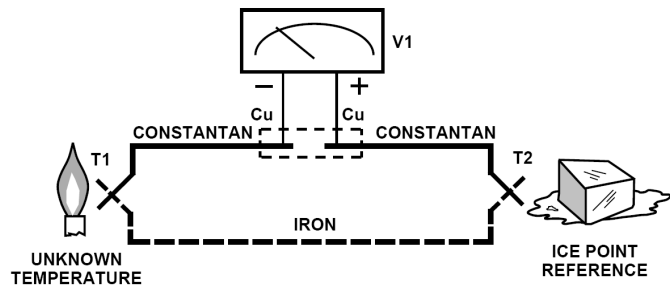


FIGURE 10: Thermocouple voltage with 0°C reference

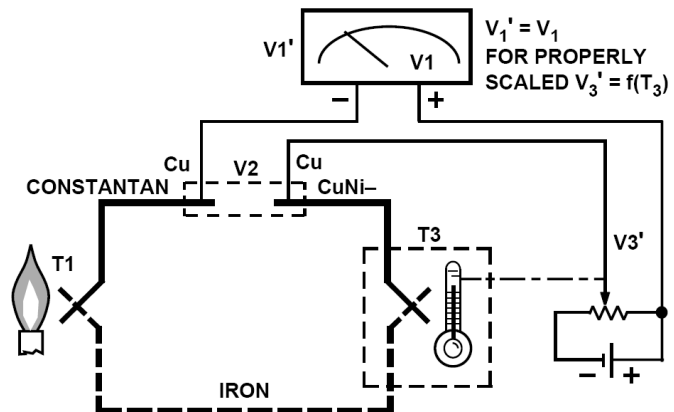


FIGURE 11: Substitution of measured reference temperature for Ice point reference

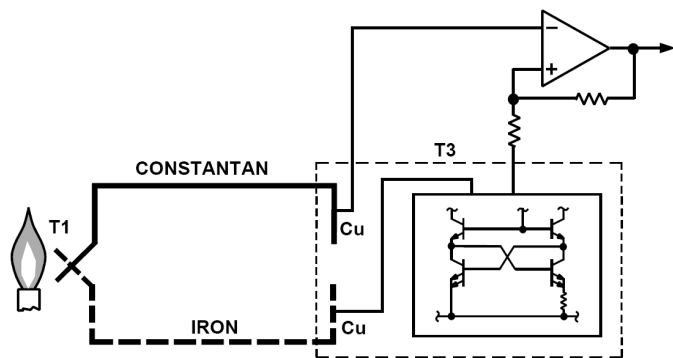


FIGURE 12: Connecting isothermal junctions

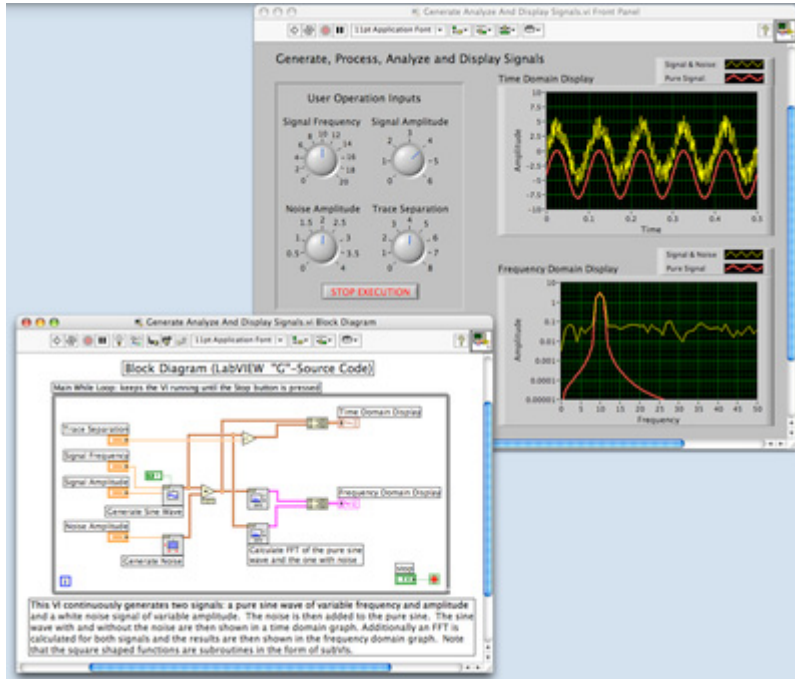


FIGURE 13: Graphical windows interface ability of LabVIEW

different electrical signals into voltage that can then be digitized using analog to digital converters (ADCs).

Analog signals tolerate almost no cross talk and so are converted to digital data, before coming close to a PC or before travelling along long cables. For analog data to have a high signal to noise ratio, the signal needs to be very high, and sending ± 10 Voltages along a fast signal path with a 50 Ohm termination requires powerful drivers. With a slightly mismatched or no termination at all, the voltage along the cable rings multiple time until it is settled in the needed precision. Digital data can have ± 0.5 Voltage. The same is true for DACs. Also digital data can be sent over glass fibre for high voltage isolation or by means of Manchester encoding or similar through RF-couplers, which prevent net hum (Wikipedia, 2007).

DAQ hardware is what usually interfaces between the signal and a PC. It could be in the form of modules that can be connected to the computer's ports (parallel, serial, USB, etc...) or cards connected to slots (PCI, ISA) in the mother board. Usually the space on the back of a PCI card is too small for all the connections needed, so an external breakout box is required. Figure 14 shows the arrangement of all units connected for data gathering process.



FIGURE 14: The arrangement of all units connected for the data gathering process

3.3 Analyzing

Simple Matlab code (appendix B) was used to analyze data gathered by Labview in text file format. To make sure that measurement is not missing any event, the sampling frequency was 10 Hz for each point. Then Matlab code calculated mean temperature within 10 seconds, to plot the temperature change during time. So the final graphs illustrate mean temperature in 10 seconds, but each point is the mean of 100 data for one point of pot.

3.4 Installation

According to previous description and Figure 9, all instruments were installed in the pot. Pc, wires, connections and software were tested before moving to field. Figure 14 shows the installation process. After installation of all units in laboratory, instruments were moved to Gardabaer to be installed in the pot. Lots of improvement has been made during this period in order to obtain more reliable data as will be described later in this chapter. Family was using the pot during the monitored periods. To have all wires stable at their planned position, stainless steel weight was fastening to end of wires. It is shown in Figure 15.

Within a few meters distance from pot, in a corner of the yard, a point with 2 m height from pot was selected to measure air temperature. Figure 16 shows the position of this point. In order to protect the thermocouple wire from the effect of wind and rain and to have more stable air flow around wire, it was put into a small pipe which was open in both ends. Addition to calibration of wires, the reliability of air temperature measurement was checked randomly with local measurement by thermometer and also from meteorological office in Reykjavik. There were some errors that were improved by changing the wire. Some of these errors will be described later in this chapter.

3.5 Results

3.5.1 Monitoring of current situation (before plate installation)

As it is explained previously, the temperature in the pot is controlled by an electric system which feeds water at a predetermined temperature into the pot. The set point is 37°C in most cases. Which means that when the temperature in the outlet of pot reaches this temperature, electronic control system will switch on the pump to feed hot water into pot, pumping will stop once the temperature reaches to the second set point, which in this case is 40°C.

Figure 17 shows water temperature in the pot at 8 locations specified in Figure 9. The ninth measurement point is air temperature. Point (c) gives minimum temperature in all over the pot's operation time, as it can be seen from Figure 17, when the outlet temperature in the pot reaches 37°C, pumping of mixed hot water with temperature around 48°C to 50°C will begin. It is clear from results that there are points in the pot that are gone below 37°C, because the sensor related to electronic unit is

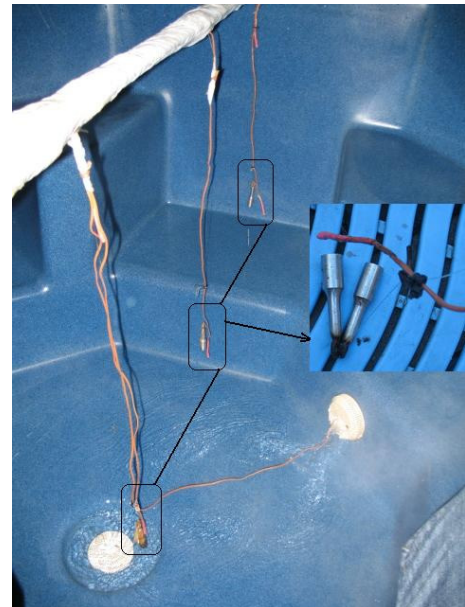


FIGURE 15: Stainless steel weight to keep wires at their right place



FIGURE 16: Air temperature measurement point

located in the outlet, point (b) is the closest measurement point to the outlet and always shows the highest temperature in the pot after point (h). This difference between points is minor and is around 1°C to 2°C. Point (win) shows the inlet water temperature. According to results and mentioned description, there are points in the pot where temperature goes down to 36°C and some times 35°C. There was one outlet point in the pot; it will have effect on symmetric assumption for temperature distribution. Points (b and h) are confirming symmetric idea with very close results, they are almost covered each other in the plots.

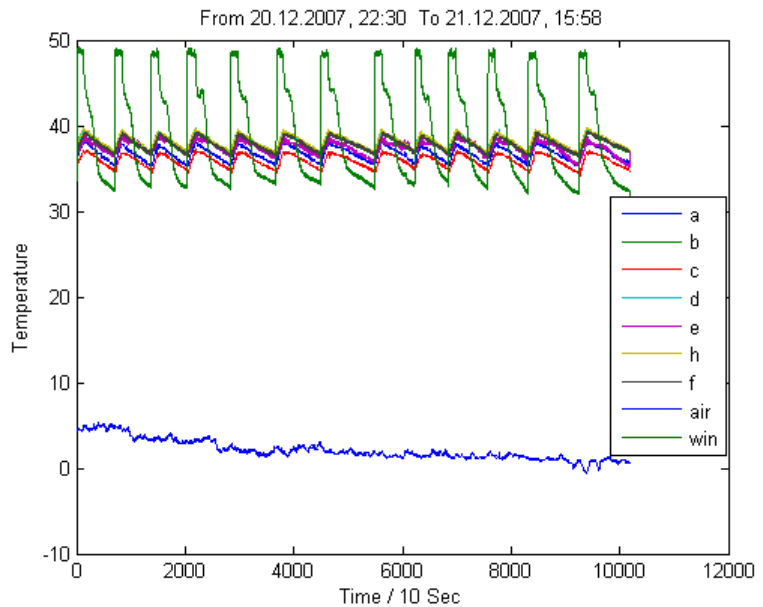


FIGURE 17: Temperature distribution in the pot including air temperature

Figure 18 shows temperature distribution in the pot in longer period while the lid is closed. There are people in the pot during Period A and B. It shows while pot is under use there is less hot water pumping into pot, which is a little confusing at first. But when some one is in the pot, there is increased mixing and sensor in outlet point is receiving higher temperature for a longer period, and because it is not long term, heat loss from pot is not affecting this event. If the lid is open for longer period than normal usage time, there will be clear effect on results. Figure 18 shows this explanation clearly.

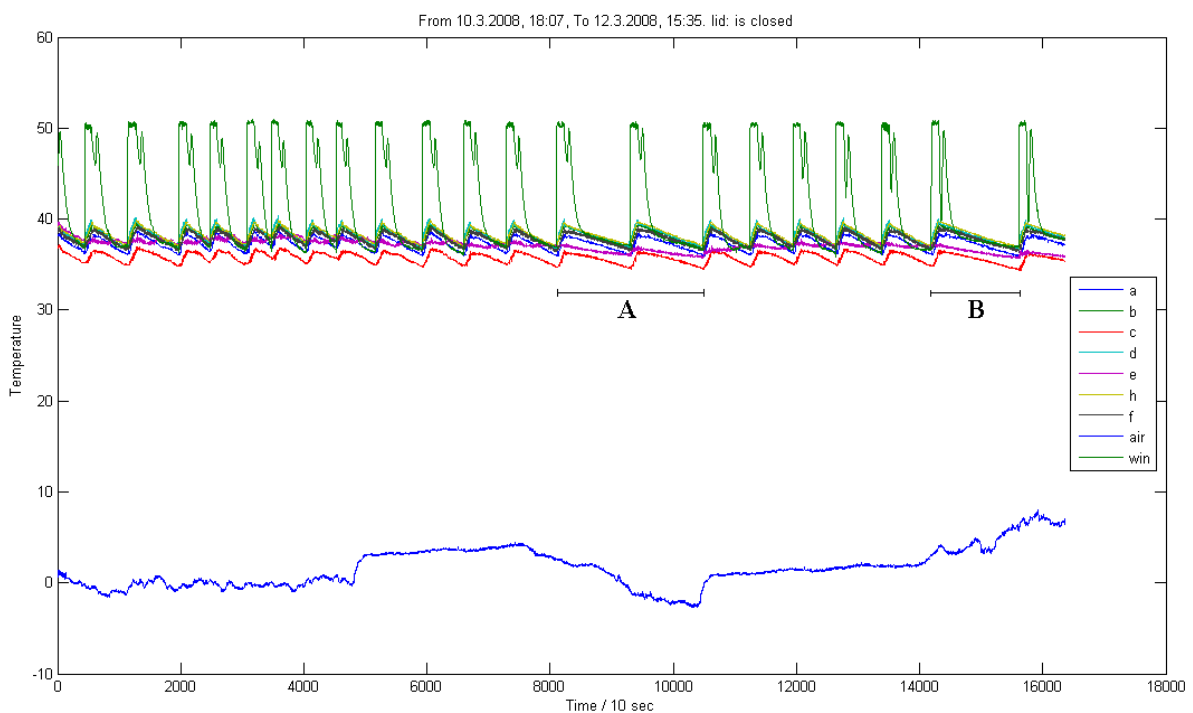


FIGURE 18: Temperature distribution in the pot for a longer period while the lid is closed

Figure 19, shows the temperature distribution in the pot while the lid is opened. This plot also monitors temperature distribution during filling of pot. The effect of open lid is clearly shown in this plot. It is rare for water inlet temperature to go below 40°C. Because the heat loss is higher in this mode and hot water pumping frequency is more. Its frequency doesn't allow water inlet temperature to cool down.

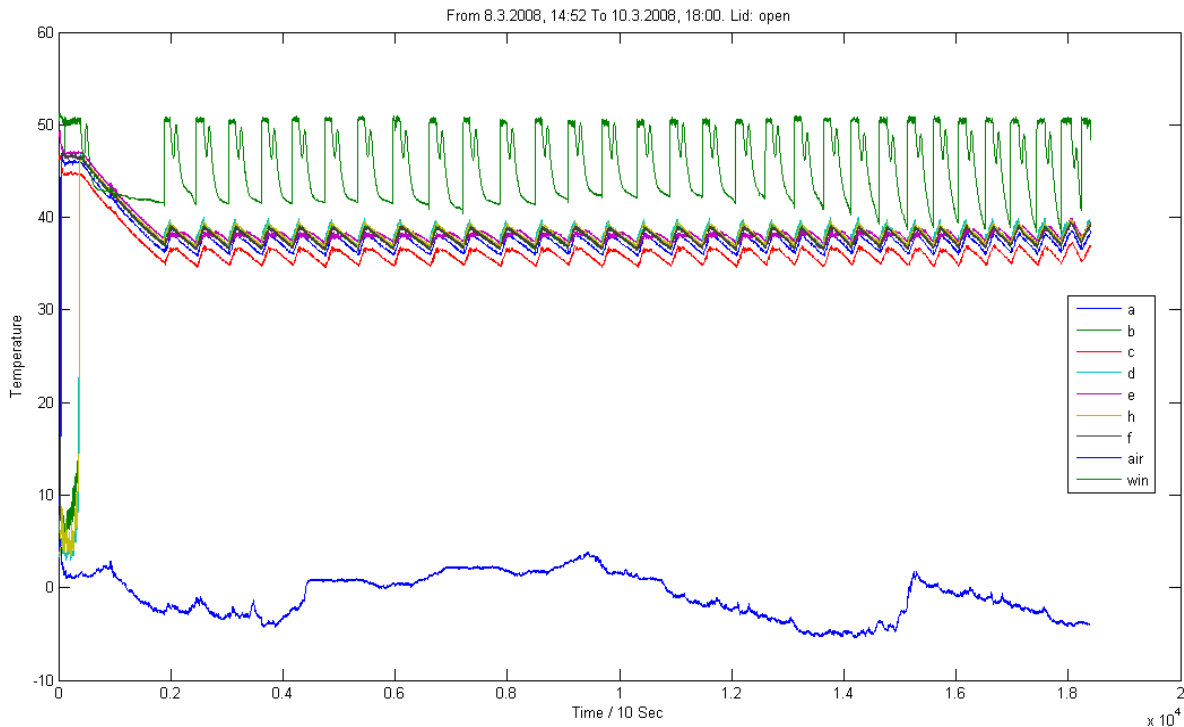


FIGURE 19: Temperature distribution in the pot for a longer period while the lid is opened

3.5.2 Monitoring with installed plate

As described in introduction, the aim of the study was to design and prove the concept of an open heat exchanger to feed hot water into the pot without mixing with cold water. The heat exchanger design is described in Heat loss chapter. The open heat exchanger plate was installed in the pot. Some changes were necessary in the plumbing and control system of pot. The cold water was disconnected. Hot water pipe was sent through pot's drainage pipe with 6.3 mm inner and 12.7 mm outer diameter of rubber pipe to feed hot water into pot from the bottom, Figure 20 displays the relationship between diameter and heat loss, pressure drop and velocity changes. It was also important to take into account the possibility of emptying of pot, because within monitoring period family was going to use the pot.

Figure 21, shows the steps of hot water piping in new system, step 1 shows the pot drainage. Step 2, illustrates how the rubber pipe has passed through drainage pipe, and step 3, displays final version of this part of installation.

Because the pot was not new, the bottom was deformed and installing the plate had some difficulties. Small slotted plastic unit (As shown in Figure 22, steps 1-3), was used to pot drainage unit. Through this unit, steel special made pipe (Figure 22, section 1) passed to connect to plate. Figure 22 shows described steps and plate views.

As the open heat exchanger can only pass a limited amount of heat, the flow must be restricted in this mode of operation. Some changes were made to the electrical unit. Figure 23a, shows how the rubber pipe is connected to electrical unit and central district heating system. Figure 23b, shows control valve to restrict flow and special digital unit to measure fluid properties.

Pipe Diameter and related parameter

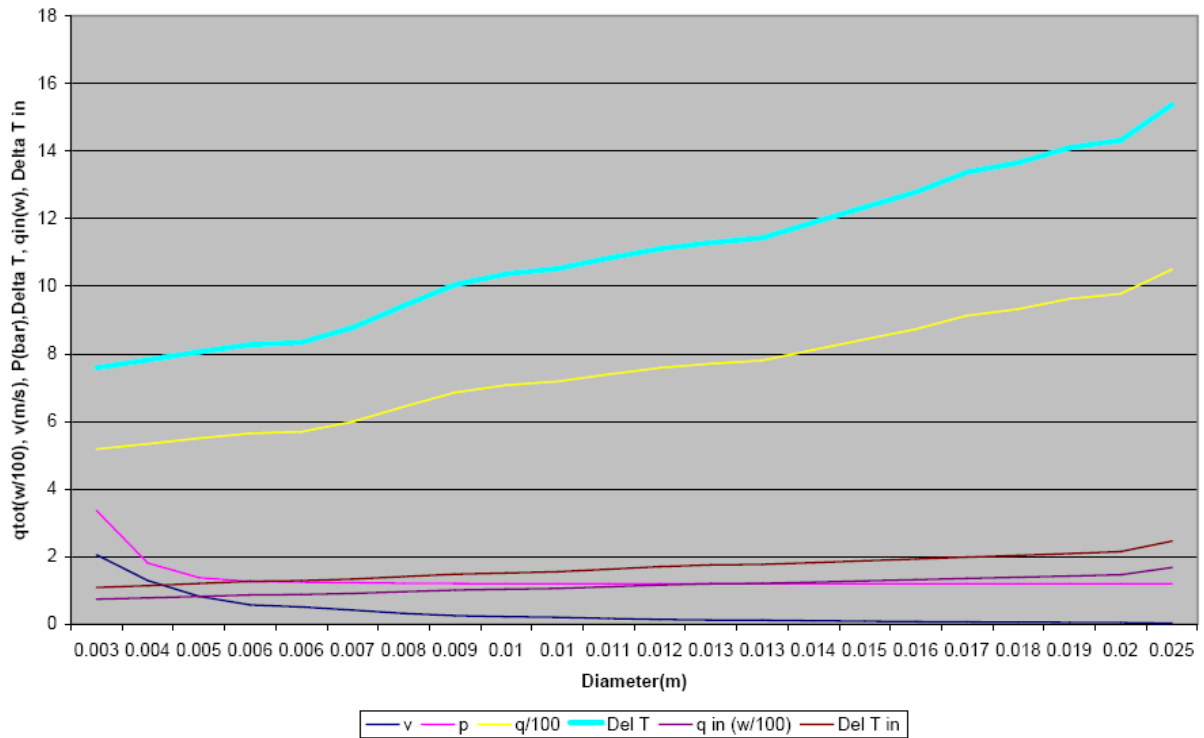


FIGURE 20: Relationship between pipe diameter and heat loss, pressure drop and velocity change

After installation of all new system measurement points were set as before, the only change was that point (win) was used to measure plate edge temperature. Other points stayed as previously explained. Electronic safety unit was adjusted to control operation mode, meaning it was possible to switch off the old system and start the new one. Then pot was filled and measurement began. At the beginning, old system was working with opened lid, after around an hour it was switched to new system. Figure 24, shows the first measurement with plate. At section N.s 2, there is suddenly change in the water inlet temperature. As it was described previously the pot was not new and the floor was very deformed, so the plate was not 100% balanced. When pot went under use, the plate moved from its balanced situation. That is why in this plot (win) point shows less temperature in section N.s 2. Figure 24, ends with few minutes of pot emptying at the end of section N.s 2.

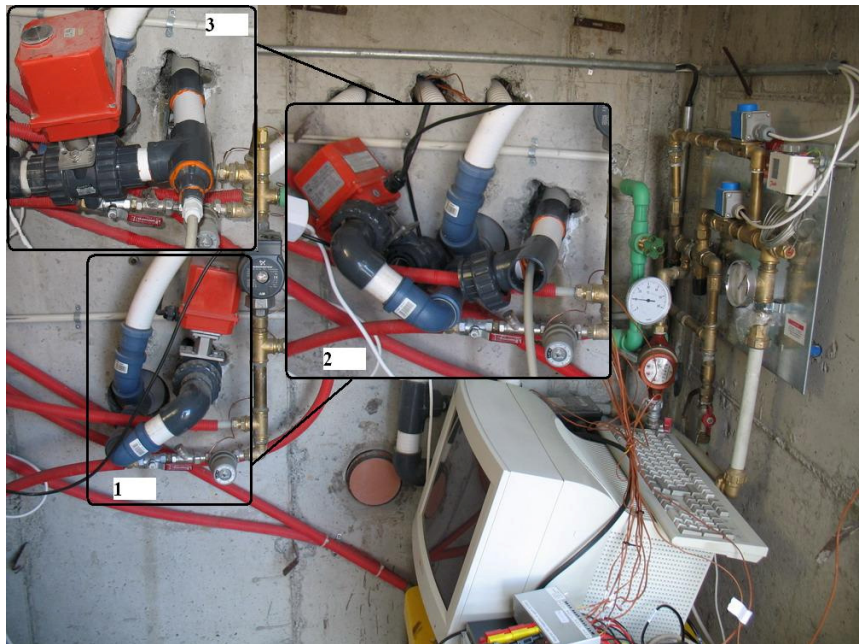


FIGURE 21: Rubber pipe installation steps using pot drainage pipe

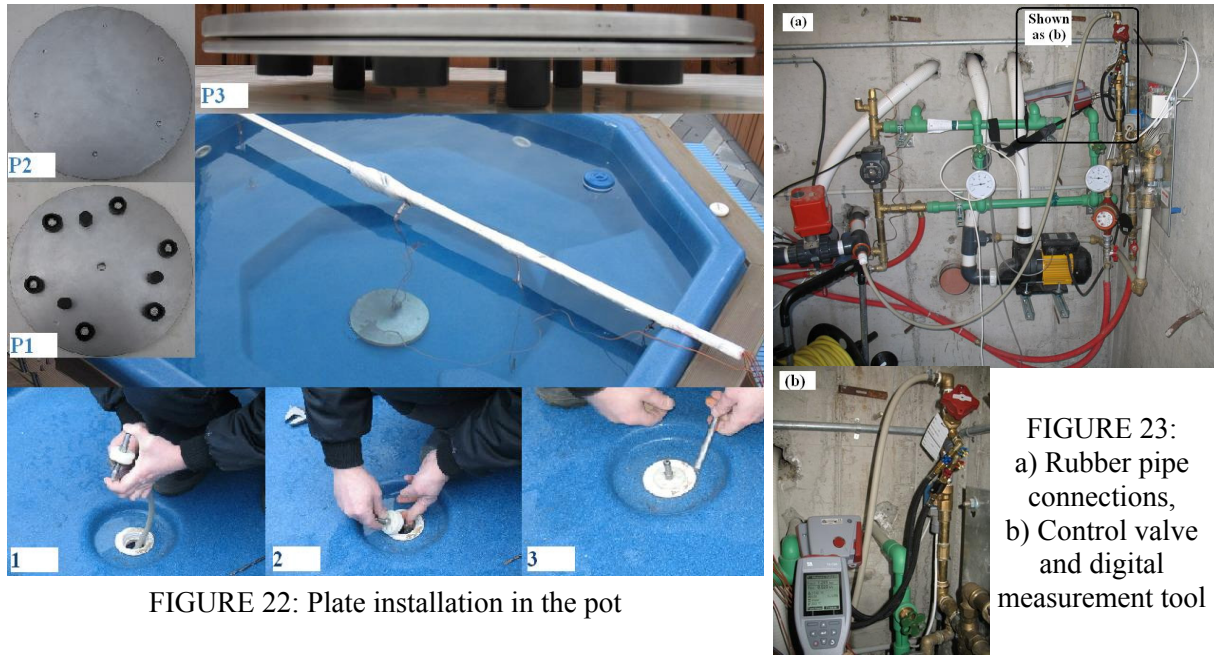
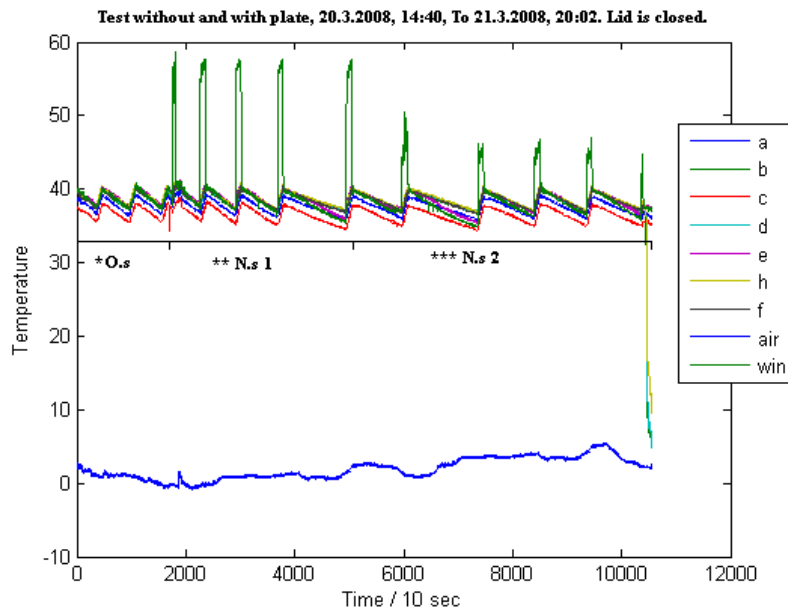


FIGURE 22: Plate installation in the pot



* O.s: Old system for one hour, rest is transferring from O.s to new one. 14:40 - 19:40 20 march 2008

** N.s 1: New system with plate from 19:40 20.3.08 to 06:20 21.3.2008

*** N.s 2: New system with plate from 06:20 to 20:02, 21 march 2008

FIGURE 24: First measurement with the plate

To investigate the effect of different mass flow rates on temperature distribution of pot and its operation, it seemed necessary to apply several mass flow rates and monitor the performance of system. At first run of measurement with open heat exchanger, by mistake mass flow rate was not taken into account, the pumping frequency was low, but the hot water temperature into pot was very high and not acceptable. The remedy was implementing a new control valve and installing a special digital unit, restricting the mass flow rate. This unit is illustrated in Figure 23.

As it is described, it was very important to understand how plate will operate with regard to mass flow rate. According to Figure 25, the logging period is 17 hours and 53 minutes, which is 6440 points in the plot. Around 1800 points are pumping period within this monitoring. This is almost equal to 5 hours operation. Then it is clear that pot is using 1800 litre hot water during 18 hours operation with 0.1 l/s mass flow rate. The operation was well enough and while family used pot, this amount of mass

flow was able to sustain desired temperature in the pot. 28% of operation time is period of pumping hot water into pot while the mass flow rate is 0.1 l/s. With assumption of having proportional relation between time and water usage, regardless of weather condition, it can be calculated that with 0.1 l/s mass flow rate, pot's hot water usage within 24 hours is equal to 2400 litres.

According to heat loss calculation 0.012 l/s was calculated value for the average hot water flow rate into pot. Figure 26 shows the pot temperature with 0.02 l/s mass flow rate. It is clear from plot that this amount of water was not able to keep pot's temperature in desired value. Of course weather temperature and wind speed are important parameters in this respect. But with this flow rate minimum temperature inside pot can go below 32°C at point c, which minimum value used to be around 35°C in normal monitoring results. It is also clear from Figure 26 that hot water was fed into pot during all period of operation with fix amount of 0.02 l/s, even though it was not enough to keep pot's temperature in acceptable range.

New system, from 26.3.2008, 16:00, 1580 m3, to 27.3.2008, 09:53, 1582 m3. Lid is closed. The flow rate is analogue but the flow rate during pumping was around 0.1 lit/s.

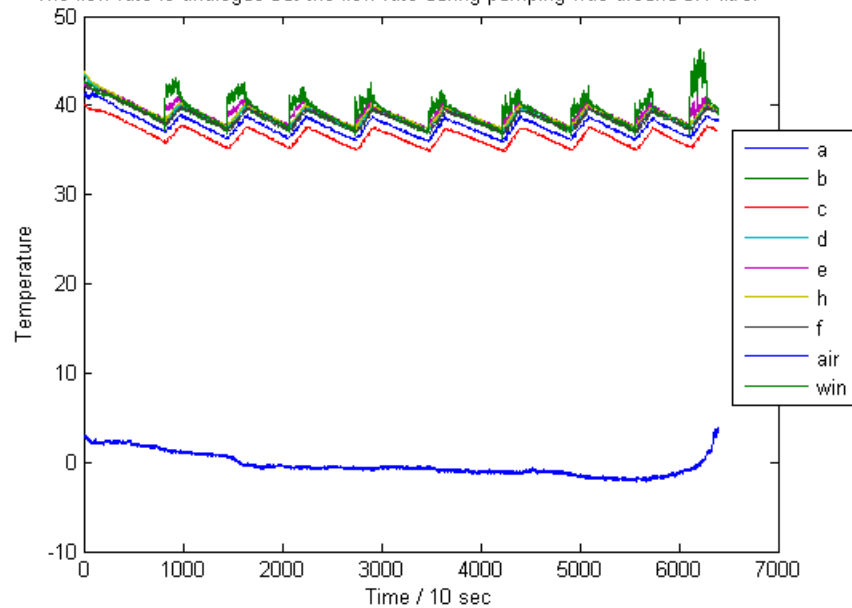


FIGURE 25: Pot temperature distribution with plate and 0.1 l/s mass flow rate

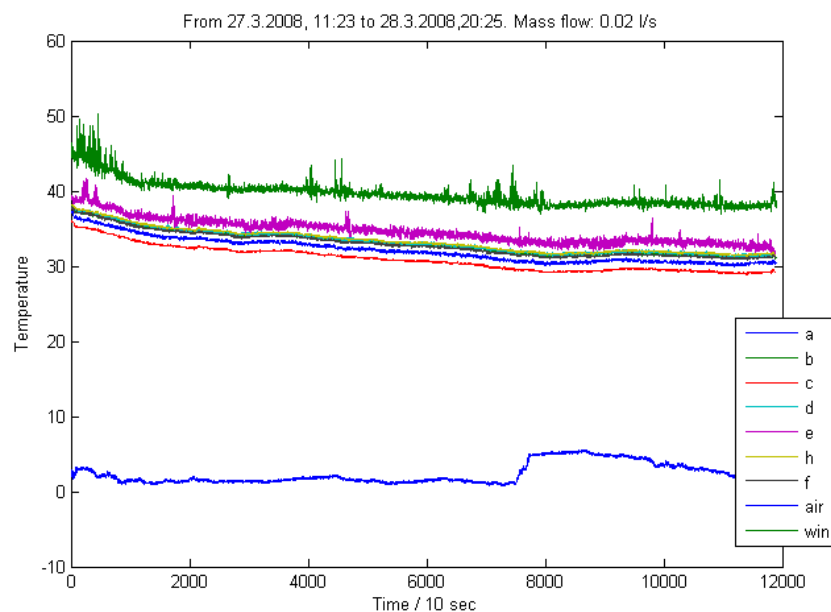


FIGURE 26: Pot temperature distribution with plate and 0.02 l/s mass flow rate

Temperature of plate itself is very important parameter, because it rests in the bottom of the pot and will be touched by the user. It should have acceptable range of temperature. With initial arrangement of measuring it was not possible to measure exactly plate's surface temperature.

With temperature loggers, as shown in Figure 27, plate's temperature was measured. Positions of points win and e were changed according to Figure 28, to measure temperature at two water inflow points. In Figure 28 first 400 points show the filling pot. It was necessary for sensors to be heated more than 70°C to begin their recording. As it was expected the minimum temperature was measured at the end, where the maximum temperature was in the centre of plate. As it is clear, 50°C is acceptable at edges of plate, but temperature at the end and middle of plate is relatively high. This

point led project to modelling of heat exchanger with different sizes of plate using Fluent software, that will be discussed in next chapter. There is correlation between mass flow rate and plate's temperature, as higher mass flow rate gives more temperature to plate.

Figures 29-34 show the temperature distribution in the pot with several mass flow rates. These plots are at the same time with sensors on plate that are shown in Figures 27 and 28. In these plots point (e) was moved from top of the plate to its side to measure water inflow temperature. Because the mass flow was restricted in low rate, the pumping was continually going on during measuring period. Except Figure 32 with 0.05 l/s mass flow rate that pumping of hot water was stopped. Digital flow measurements begins to work while there is pumping, also sensors had just 10 hours time limitation to work. For more efficient utilization of sensors and trying other range of mass flow, artificially pump was forced to work; it can be done by removing some water from or adding cold water into pot.



FIGURE 27: Plate logging arrangement

Temperature at different points of plate's surface with different flow rates

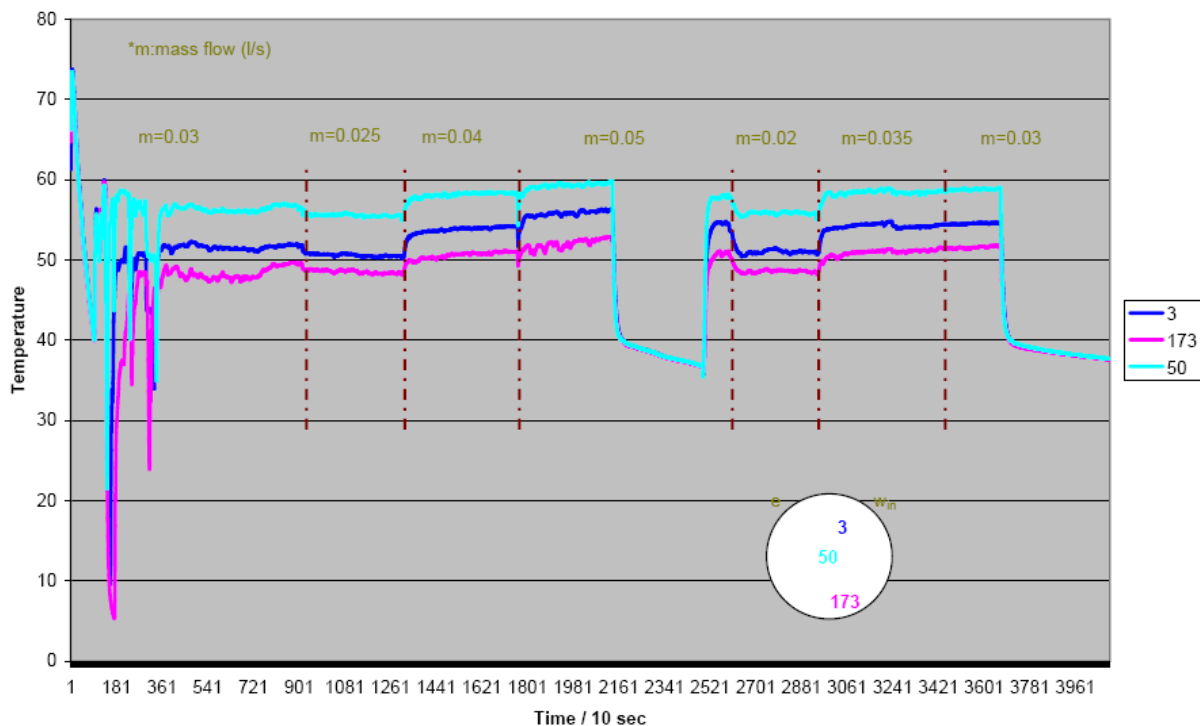


FIGURE 28: Temperature distribution in the surface of plate within different mass flow rates

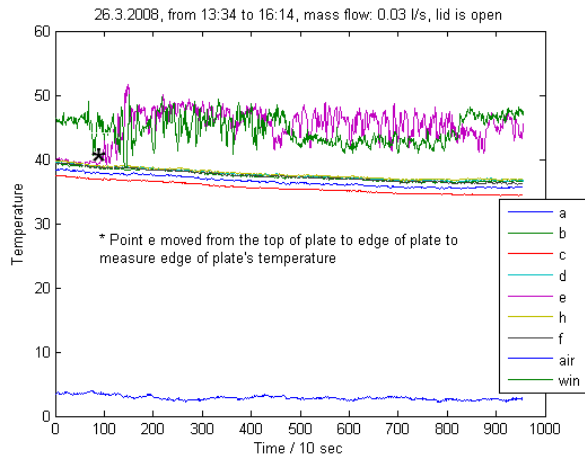


FIGURE 29: Temperature distribution in the pot with 0.03 l/s mass flow rate

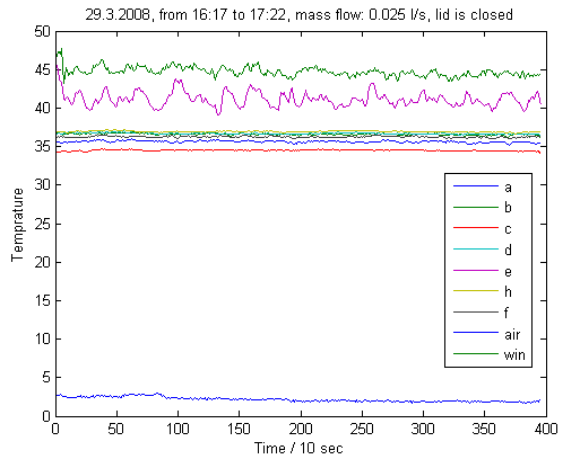


FIGURE 30: Temperature distribution in the pot with 0.025 l/s mass flow rate

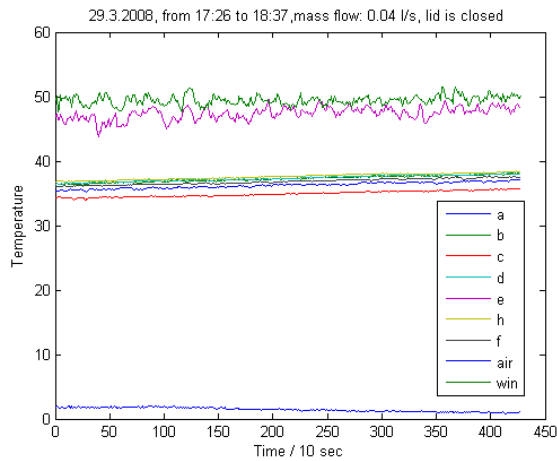


FIGURE 31: Temperature distribution in the pot with 0.04 l/s mass flow rate

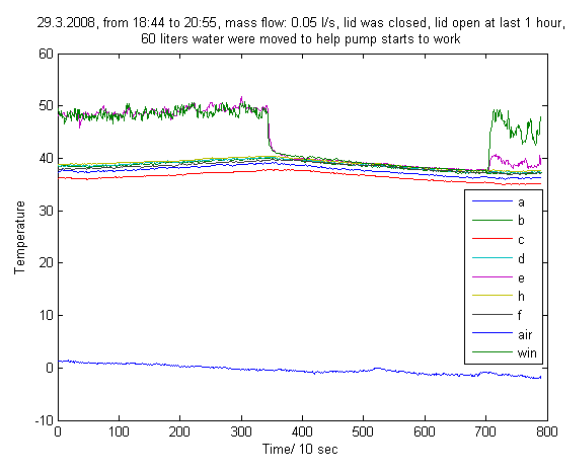


FIGURE 32: Temperature distribution in the pot with 0.05 l/s mass flow rate

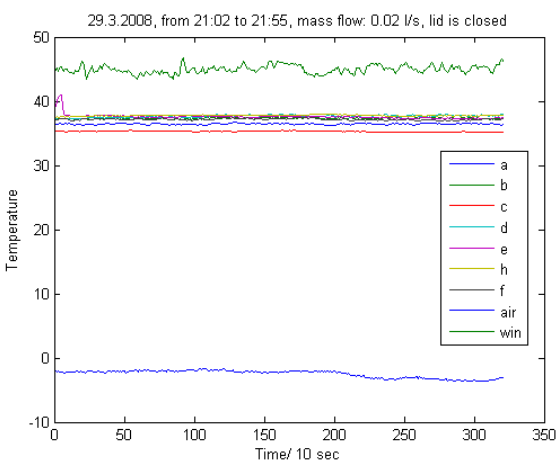


FIGURE 33: Temperature distribution in the pot with 0.02 l/s mass flow rate

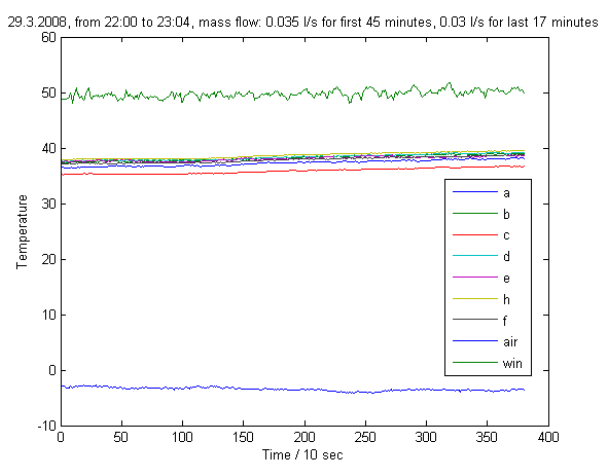


FIGURE 34: Temperature distribution in the pot with 0.035 l/s and 0.03 l/s mass flow rate

After all investigations and applying several mass flow rates to feed hot water into pot, it was decided to choose 0.03 l/s as an accepted value for mass flow. Figure 35, shows 67% of operation time is period of pumping hot water into pot while the mass flow rate is 0.03 l/s. With assumption of having proportional relation between time and water usage, regardless weather condition, it can be calculated that with 0.03 l/s mass flow rate, pot's hot water usage within 24 hours is equal to 1728 litres.

From 29.3.2008, 23:05 to 30.3.2008, 16:48, mass flow: 0.03 l/s, pressure 1.1 bar, lid is closed, results show 12 hours hot water pumping within 18 hours

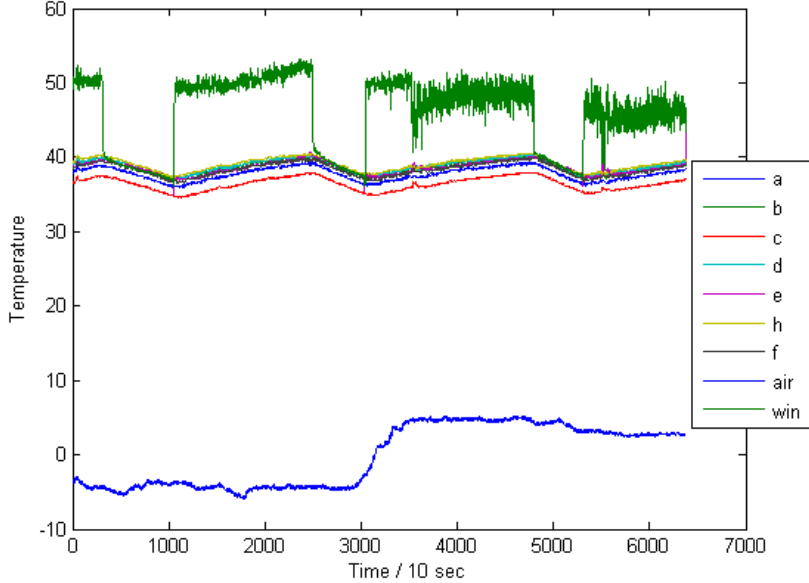


FIGURE 35: Temperature distribution in the pot with 0.03 l/s mass flow rate

3.6 Errors

Power source: Amplifier boxes need power; at first monitoring it was found that there were some unexpected values for temperature in the pot (-40 °C inside pot), which was absolutely wrong. Firstly all points were checked, and then it was proven that lower power will deliver more inaccurate data. The power sources were batteries with 9v. After more investigation it was clear that DC current is not enough to be used as a power source for long term logging. Then AC to DC transformer was installed in the system and problem was solved.

To make sure that data are accurate, calibration was done at field situation. The results are illustrated at Table 12. The analogue data are according mean data from thermometer and digital values are according to mean value from Labview and analyzed by Matlab code. The positive correction values were added to measured values and the negative values were subtracted.

TABLE 12: The result of calibration

Wires	Analogue	Digital	Correction value
A	90.04	89.61	0.43
B	88.91	89.03	-0.12
C	88.22	87.24	0.98
D	86.85	87.92	-1.07
E	85.96	87.34	-1.37
F	92.91	92.89	0.01
H	94.2	95.28	-1.08
Win	84.8	85.44	-0.64

When accuracy of all measurement instruments was tested, one unexpected problem has happened. The graph was totally strange and water consumption was extremely high. It was found out that electronic control unit in pot had problem. Figure 36 shows this error. This plot is totally different from others and it shows 31 m³ water consumption within 46 hours.

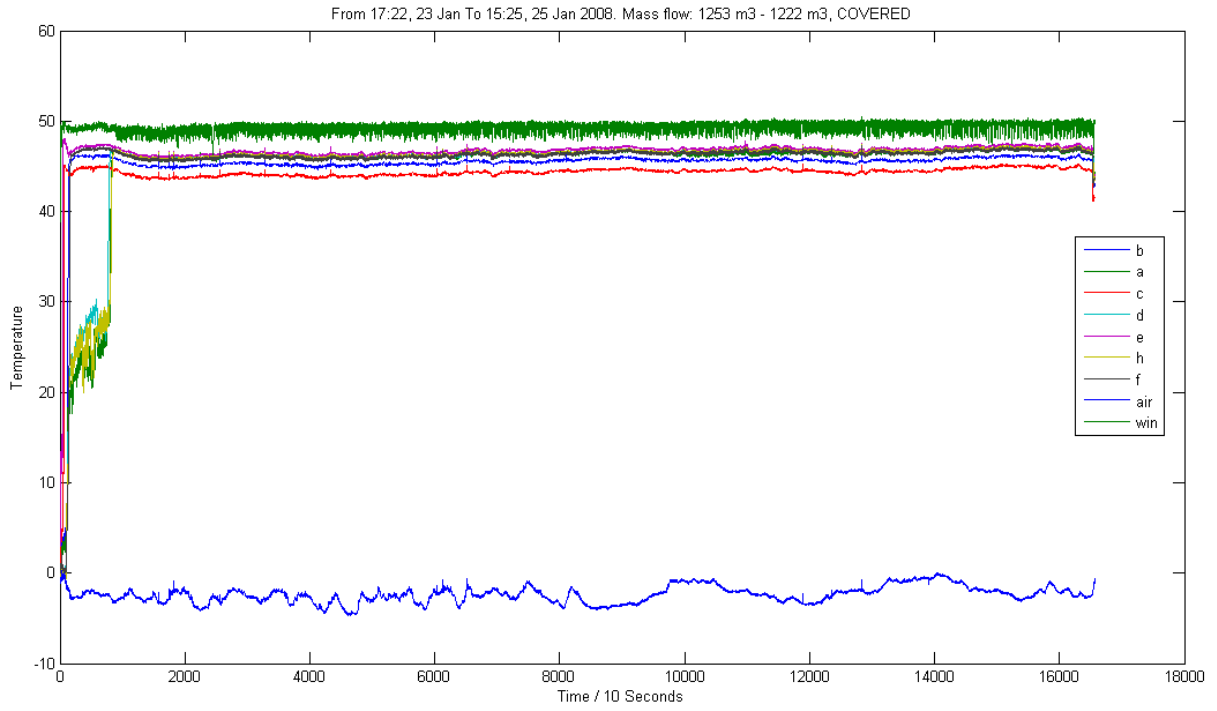


FIGURE 36: Due to error in the electronic control unit the water consumption within the 46 hours is shown as 31 m³

4. MODELLING

4.1 Introduction

In previous chapters discussion was done about heat transfer and its related topics. As it was mentioned heat transfer can occur by three main methods: conduction, convection, and radiation. Physical models involving conduction, convection only are the simplest, while buoyancy-driven flow or natural convection, and radiation models are more complex. Depending on problem, FLUENT will solve a variation of the energy equation that takes into account the heat transfer methods that have been specified. Information about heat transfer theory and how to setup and use heat transfer in FLUENT model is presented in the following subsections:

4.2 Heat transfer theory

4.2.1 The energy equation

FLUENT solves the energy equation in the following form (Fluent, 2008):

$$\frac{\partial}{\partial t}(\rho E) + \nabla \cdot (\bar{v}(\rho E + p)) = \nabla \cdot (k_{eff} \nabla T - \sum_j h_j \vec{J}_j + (\bar{\tau}_{eff} \cdot \bar{v})) + S_h \quad (4.1)$$

Where k_{eff} is the effective conductivity ($k + k_t$, where k_t is the turbulent thermal conductivity, defined according to the turbulence model being used), and \vec{J}_j is the diffusion flux of species j . The first three terms on the right-hand side of Equation 4.1 represent energy transfer due to conduction, species diffusion, and viscous dissipation, respectively. S_h includes the heat of chemical reaction, and any other volumetric heat sources that have been defined.

In Equation 4.1,

$$E = h - \frac{p}{\rho} + \frac{v^2}{2} \quad (4.2)$$

Where sensible enthalpy h is defined for ideal gases as:

$$h = \sum_j Y_j h_j \quad (4.3)$$

and for incompressible flows as:

$$h = \sum_j Y_j h_j + \frac{p}{\rho} \quad (4.4)$$

In Equations 4.3 and 4.4, Y_j is the mass fraction of species j and:

$$h_j = \int_{T_{ref}}^T C_{p,j} dT \quad (4.5)$$

where T_{ref} is 298.15 K.

Inclusion of pressure work and kinetic energy terms. Equation 4.1 includes pressure work and kinetic energy terms which are often negligible in incompressible flows. For this reason, the pressure-based solver by default does not include the pressure work or kinetic energy when incompressible flow is being solved. To include these terms the energy tab from models should be turned on in defining process.

Pressure work and kinetic energy are always accounted for when the aim is to model compressible flow or using the density-based solver.

Inclusion of the species diffusion term. Equation 4.1 includes the effect of enthalpy transport due to species diffusion. When the pressure-based solver is used, the term in Equation 4.6 is included in Equation 4.1 by default. When the density-based solver is used, this term is always included in the energy equation:

$$\nabla \cdot (\sum_j h_j \vec{J}_j) \quad (4.6)$$

Energy sources. Sources of energy, S_h , in Equation 4.1 includes the source of energy due to chemical reaction, When one of the radiation models is being used, S_h in Equation 4.1 also includes radiation source terms. It should be noted that the energy sources, S_h , also includes heat transfer between the continuous and the discrete phase.

Diffusion at inlets. The net transport of energy at inlets consists of both the convection and diffusion components. The convection component is fixed by the inlet temperature. The diffusion component, however, depends on the gradient of the computed temperature field. Thus the diffusion component (and therefore the net inlet transport) is not specified a priori.

In some cases, it is possible to specify the net inlet transport of energy rather than the inlet temperature. If the pressure-based solver is being used, it can be done by disabling inlet energy diffusion. By default, FLUENT includes the diffusion flux of energy at inlets. Energy tab in models function is controlling this item. Inlet diffusion cannot be turned off if the density-based solver is being used.

4.2.2 Natural convection and buoyancy - driven flows

When heat is added to a fluid and the fluid density varies with temperature, a flow can be induced due to the force of gravity acting on the density variations. Such buoyancy-driven flows are termed natural-convection (or mixed-convection) flows and can be modelled by FLUENT.

Theory. The importance of buoyancy forces in a mixed convection flow can be measured by the ratio of the Grashof and Reynolds numbers:

$$\frac{Gr}{Re^2} = \frac{g\beta\Delta TL}{\nu} \quad (4.7)$$

When this number approaches or exceeds unity, buoyancy will contribute to the flow. Conversely, if it is very small, buoyancy forces may be ignored in simulation. In pure natural convection, the strength of the buoyancy-induced flow is measured by the Rayleigh number:

$$Ra = \frac{g\beta\Delta TL^3 \rho}{\mu\alpha} \quad (4.8)$$

where β is the thermal expansion coefficient:

$$\beta = -\frac{1}{\rho} \left(\frac{\partial \rho}{\partial T} \right)_p \quad (4.9)$$

and α is the thermal diffusivity:

$$\alpha = \frac{k}{\rho C_p} \quad (4.10)$$

Rayleigh numbers less than 10^8 indicate a buoyancy-induced laminar flow, with transition to turbulence occurring over the range of $10^8 < Ra < 10^{10}$.

4.3 Modelling natural convection in a closed domain

To model natural convection inside a closed domain, the solution will depend on the mass inside the domain. Since this mass will not be known unless the density is known, the flow should be modelled in one of the following ways:

Perform a transient calculation. In this approach, the initial density will be computed from the initial pressure and temperature, so the initial mass is known. As the solution progresses over time, this mass will be properly conserved. If the temperature differences in domain are large, this approach must be followed.

Perform a steady-state calculation using the Boussinesq model. In this approach, a constant density will be specified, so the mass is properly specified. This approach is valid only if the temperature differences in the domain are small; if not, the transient approach must be used.

4.3.1 The Boussinesq model

For many natural-convection flows, the Boussinesq model gives faster convergence rather than setting up the problem with fluid density as a function of temperature. This model treats density as a constant value in all solved equations, except for the buoyancy term in the momentum equation:

$$(\rho - \rho_0)g \approx -\rho_0\beta(T - T_0)g \quad (4.11)$$

where ρ_0 is the (constant) density of the flow, T_0 is the operating temperature, and β is the thermal expansion coefficient.

Equation 4.11 is obtained by using the Boussinesq approximation $\rho = \rho_0 (1 - \beta\Delta T)$ to eliminate ρ from the buoyancy term. This approximation is accurate as long as changes in actual density are small; specifically, the Boussinesq approximation is valid when $\beta(T - T_0) \ll 1$.

Operating density. When the Boussinesq approximation is not used, the operating density ρ_0 appears in the body-force term in the momentum equations as $(\rho - \rho_0)g$.

This form of the body-force term follows from the redefinition of pressure in FLUENT as:

$$p'_s = p_s - \rho_0 gx \quad (4.12)$$

The hydrostatic pressure in a fluid at rest is then:

$$p'_s = 0 \quad (4.13)$$

Limitations of the Boussinesq Model. The Boussinesq model should not be used if the temperature differences in the domain are large. In addition, it cannot be used with species calculations, combustion, or reacting flows.

4.4 GAMBIT

GAMBIT is the software to create geometry and meshing. GAMBIT's single interface for geometry creation and meshing brings together most of Fluent's preprocessing technologies in one environment. This software was used to create the geometry, meshing and defining boundary conditions in all modelling process. Figures 37 and 38 show the samples of meshes were made by Gambit.

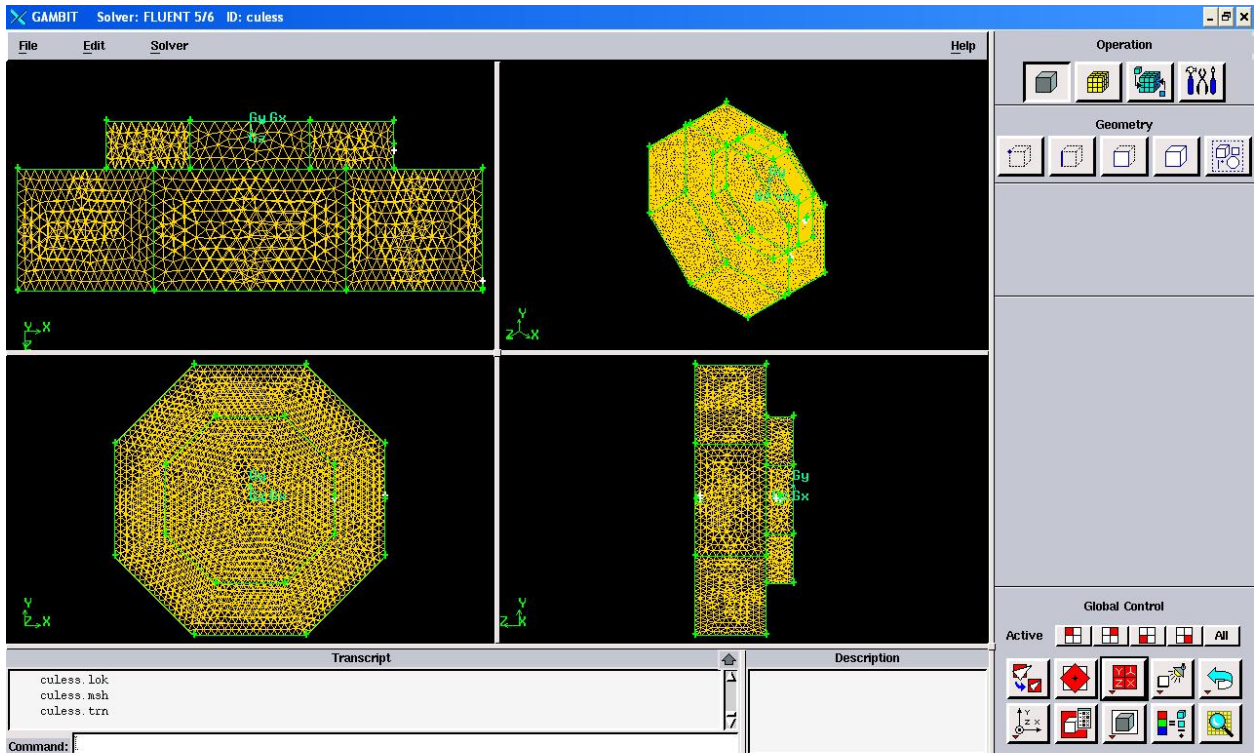


FIGURE 37: 3D mesh for whole pot

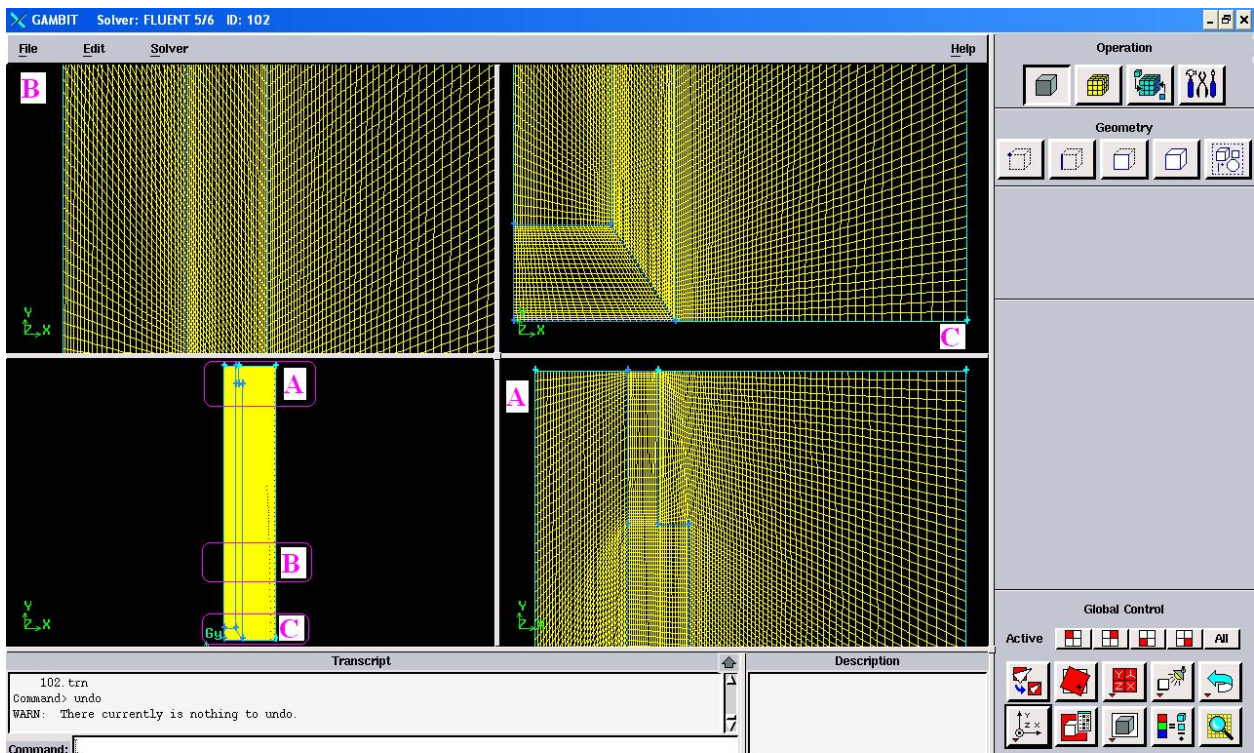


FIGURE 38: 2D mesh for plate

4.5 Results and discussions

4.5.1 Modelling of pot according to current situation

A pot according to the specifications in measurement chapter was modelled by fluent, geometry and meshing were created using Gambit including the boundary conditions. Figure 37, illustrates the created geometry and mesh. Then the file was imported to Fluent and heat transfer modelling process was applied. Table 13, shows heat transfer values in different zones and as it can be seen the value of net heat transfer is very small, which proves that the modelling has minimum possible errors. It was one of the main tools to control the reliability of the model; the closest value to zero shows more accuracy for results.

TABLE 13: Heat transfer values in different zones

Zones	Value
Zone 6 (inlet)	2078.34
Zone 5 (outlet)	-890.33
Zone 3 (top)	-141.77
Zone 4 (wall)	-1045.8
Net heat-transfer	0.44

Table 14, shows the average temperature at different zones of pot, 37°C is the average temperature in most zones and shows good agreement with results from monitoring.

TABLE 14: The average temperature at different zones in Kelvin

Zones	Static temperature (K)
Default-interior	308.72
Inlet	309.6
Outlet	306.46
Plane-5	310.31
Plane-6	309.64
Top	306.80
Wall	301.68
Net	308.52

Table 15, shows the maximum temperature at different parts of pot. Top, walls and outlet zones have similar temperature close to 37°C. This is in good agreement with real situation. Plane-5 and Plane-6 zones are cross sectional lines through pot, from one end to another one. The plane-5 shows higher value, due to its close position relative to water inlet point.

TABLE 15: The maximum temperature at different parts of pot

Zones	Static temperature (K)
Inlet	322.48
Outlet	309.1
Plane-5	322.48
Plane-6	312.26
Top	310.88
Wall	311.47
Net	322.48

Figure 39, shows the cross-sectional view of pot regarding to temperature distribution. It shows the water inlet point at its left side. There is good agreement in all plots compare to results from measurements. Figure 40 shows the cross-sectional view of pot, vertical to water inlet line. This figure satisfies pot's symmetric situation in good correlation. Figures 41-44, show the temperature distribution of pot in several views, in all these plots there are good agreement with measurement results.

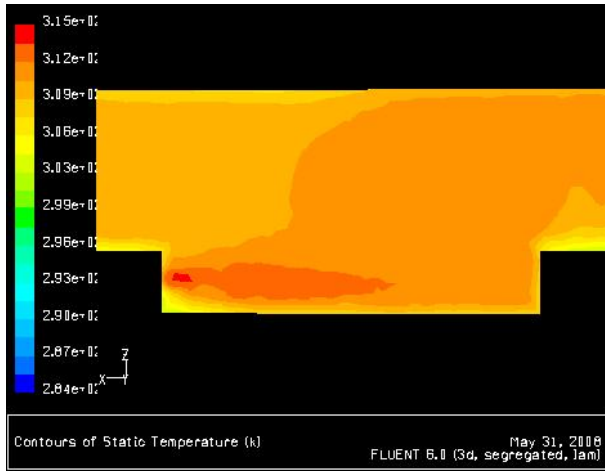


FIGURE 39: Cross-sectional view of pot, water inlet in the left side

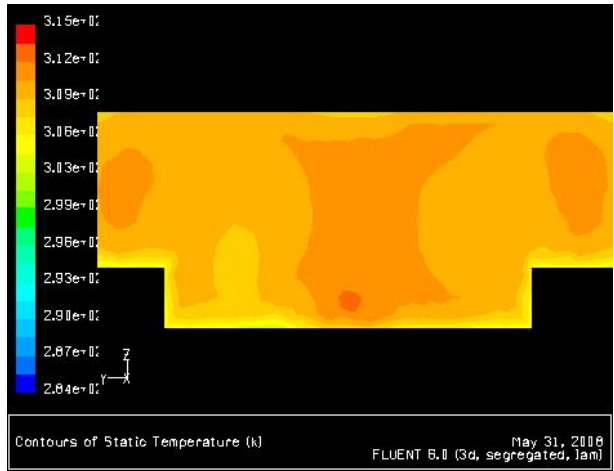


FIGURE 40: Cross-sectional view of pot, water vertical to water inlet line

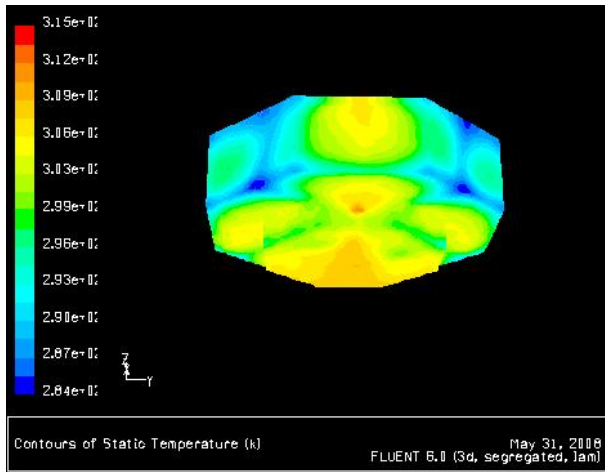


FIGURE 41: Temperature distribution in the pot

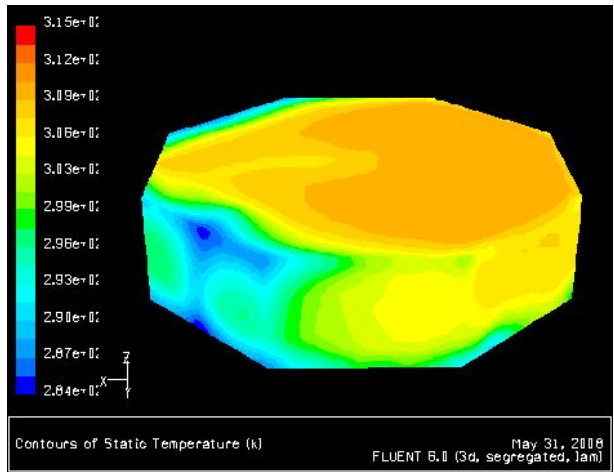


FIGURE 42: Temperature distribution in the pot

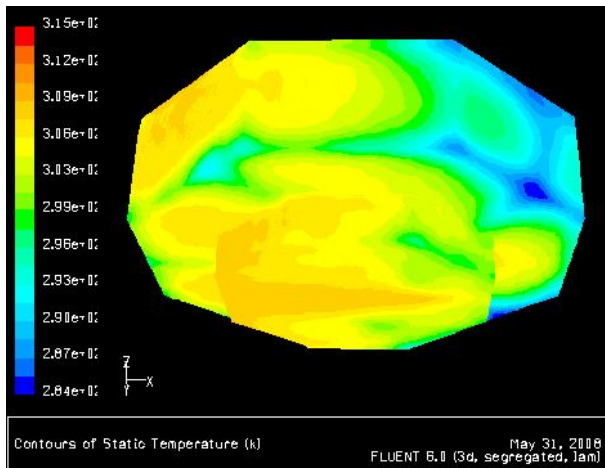


FIGURE 43: Temperature distribution in the pot

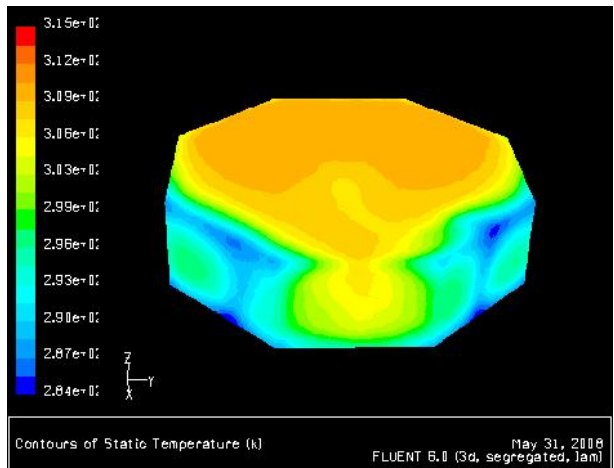


FIGURE 44: Temperature distribution of pot in different views

4.5.2 Modelling of pot with installed plate

Mass flow rate: $m=0.018$ kg/s

After modelling the current situation for pot, the results were in good agreement with measurements which has been done in pot, and then the same method has been applied to model the pot with plate. Geometry and meshing were created using Gambit including specifying the boundary conditions. Then the file imported to Fluent and heat transfer modelling process was applied. Table 16 shows heat transfer values in different zones and as it can be seen the value of net heat transfer is very small, which proves that the modelling has minimum possible errors.

TABLE 16: Heat transfer values in different zones

Zones	Values
Zone 7 (inflow)	3922.32
Zone 6 (out)	-2201.8
Zone 5 (plate)	-44.94
Zone 4 (top)	-535.05
Zone 3 (wall)	-1140.89
Net heat-transfer	-0.36

Table 17, shows the average temperature at different zones in Kelvin. The plate surface has 52°C, which is a little higher than its acceptable value (50°C). The same applies for cross sectional lines and the average temperatures are in good ranges and close agreement with measurement data. But it is necessary to check maximum temperatures in different parts of pot.

TABLE 17: Average temperature at different zones in Kelvin

Zones	Static temperature (K)
Centre	327.52
Default-interior	323.93
Inflow	343.11
Out	325.49
Plane-7	326.56
Plate	325.22
Top	311.52
Wall	304.57
Net	323.56

Table 18, shows the maximum temperature at different parts of pot. Top and outlet zones have similar temperature close to 57°C. This temperature is high and needs to be adjusted by using different mass flow rates and different plate sizes.

TABLE 18: The maximum temperature at different parts of pot

Zones	Static temperature (K)
Centre	349.85
Default-interior	349.98
Inflow	349.98
Out	329.26
Plane-7	349.79
Plate	334.94
Top	330.99
Wall	349.85
Net	349.98

Figure 45 shows the cross-sectional view of pot regarding to temperature distribution. Two vertical cross sectional lines are shown in this figure. It is interesting to see the effect of water outflow and how interrupts pot's symmetric situation. Figure 46-49, show the temperature distribution of pot in several views, the temperatures are high in most cases and needs to be adjusted as it was explained.

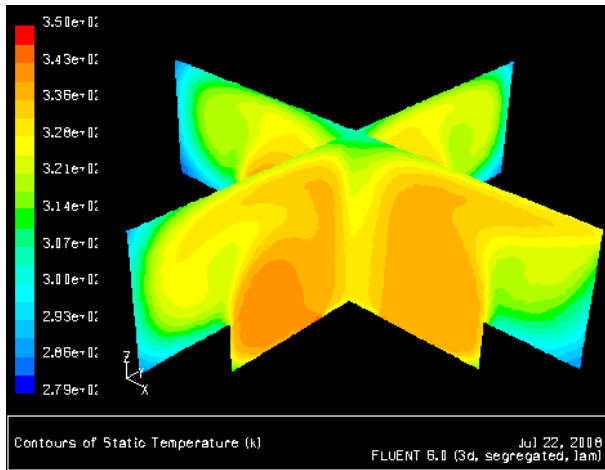


FIGURE 45: The cross sectional view of pot regarding to temperature distribution

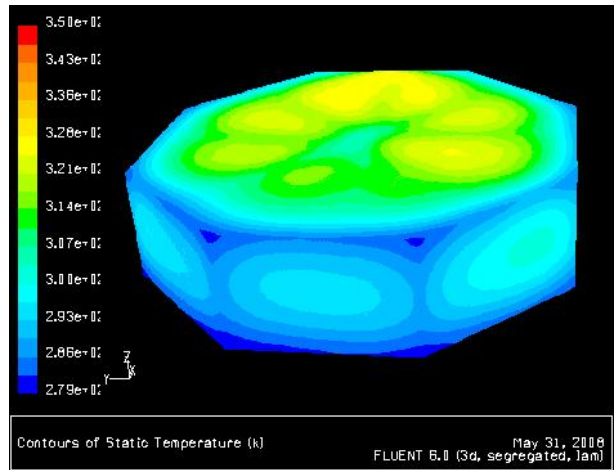


FIGURE 46: Temperature distribution in the pot

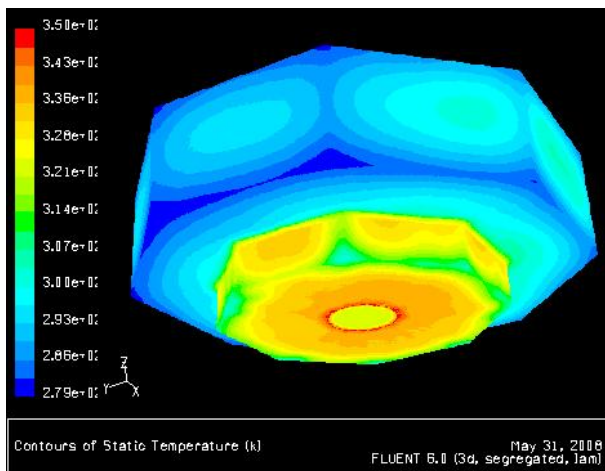


FIGURE 47: Temperature distribution in the pot

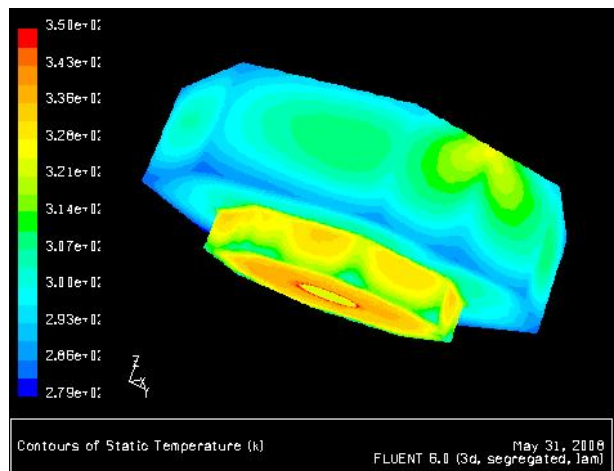


FIGURE 48: Temperature distribution in the pot

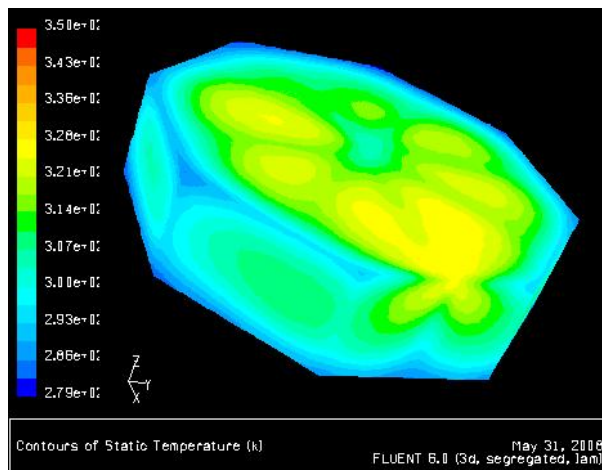


FIGURE 49: Temperature distribution in the pot

Mass flow rate: $m=0.008$ kg/s

To analyse how the pot is operating with different mass flows, the mass flow was fixed at 0.008 kg/s. Geometry, meshing and boundary condition were the same as former modelling. Table 19, shows heat transfer values in different zones and as it can be seen the value of net heat transfer is very small, which proves that the modelling has minimum possible errors.

Table 20, shows the average temperature at different zones in Kelvin. The plate surface has 52°C, which is a little higher than its acceptable value (50°C). The same applies for cross sectional lines and the average temperatures are in good ranges and close agreement with measurement data. But it is necessary to check maximum temperatures in different parts of pot.

TABLE 19: Heat transfer values in different zones

Zones	Values
Zone 7 (inflow)	1734.64
Zone 6 (out)	-827.82
Zone 5 (plate)	-40.77
Zone 4 (top)	-126.03
Zone 3 (wall)	-740.13
Net heat-transfer	-0.11

TABLE 20: The average temperature at different zones of pot

Zones	Static Temperature (K)
Centre	319.96
Default-interior	315.22
Inflow	342.96
Out	319.03
Plane-7	326.18
Plate	325.22
Top	303.10
Wall	293.48
Net	314.85

Table 21, shows the maximum temperature at different parts of pot. Top zone has temperature close to 57°C. With new mass flow rate 4°C less temperature can be seen in outlet zone. Temperature in outlet zone is about 52°C.

TABLE 21: The maximum temperature at different zones of pot

Zones	Static Temperature (K)
Centre	349.64
Default-interior	349.88
Inflow	349.88
Out	325.13
Plane-7	349.57
Plate	336.92
Top	330.57
Wall	349.72
Net	349.88

Figure 50, shows the cross sectional view of pot regarding to temperature distribution. Two vertical cross sectional lines are shown in this figure. It is interesting to see the effect of water outflow and how interrupts pot's symmetric situation.

Figures 51 and 52, show the temperature distribution of pot in different views, the temperatures are high in most cases and need to be adjusted as it was explained. Another result from these modelling is that pot gets cooler while the mass flow goes below specific mass flow rate. These cooling are clear in boundary areas.

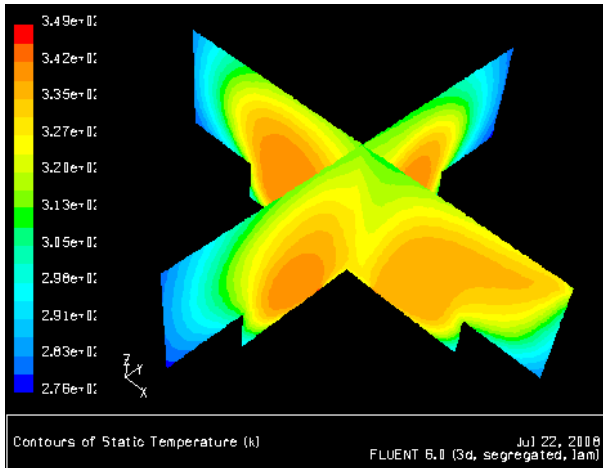


FIGURE 50: the cross-sectional view of pot regarding to temperature distribution

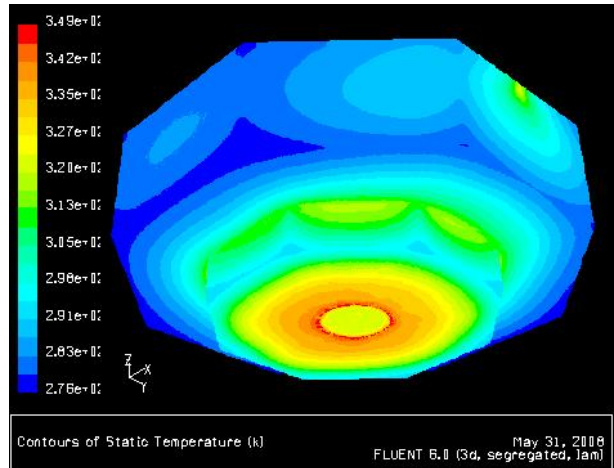


FIGURE 51: Temperature distribution in the pot

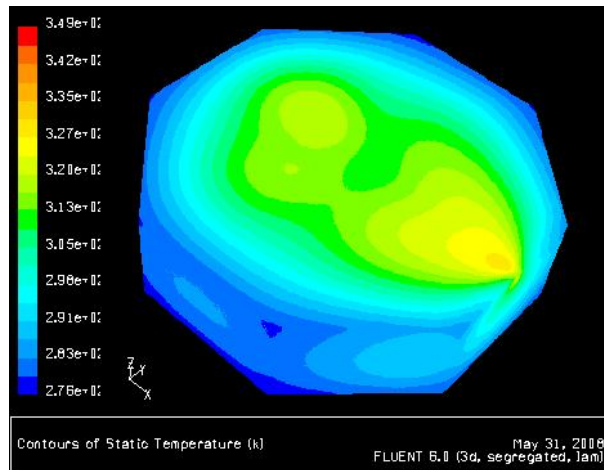


FIGURE 52: Temperature distribution in the pot

Mass flow rate: $m=0.005$ kg/s

For more analyzing of mass flow effect on pot's operation, 0.005 mass flow rates were applied. Geometry, meshing and boundary condition were the same as former modelling. Table 22, shows heat transfer values in different zones and as it can be seen the value of net heat transfer is very small, which proves that the modelling has minimum possible errors.

Table 23, shows the average temperature at different zones in Kelvin. The plate surface has 52°C, which is a little higher than its acceptable value (50°C). The same applies for cross sectional lines and the average temperatures are in good ranges and close agreement with measurement data. Average temperature in cross sectional lines is in acceptable ranges, but in top zone there is clear cooling below to 13°C which shows the mass flow rate is too low.

TABLE 22: Heat transfer values in different zones

Zones	Values
Zone 7 (inflow)	1084.21
Zone 6 (out)	-323.11
Zone 5 (plate)	-41.85
Zone 4 (top)	-190.07
Zone 3 (wall)	-529.30
Net heat-transfer	-0.13

TABLE 23: The average temperature at different zones of pot in Kelvin

Zones	Static temperature (K)
Centre	311.27
Default-interior	305.83
Inflow	342.86
Out	309.91
Plane-7	318.67
Plate	325.22
Top	286.68
Wall	287.64
Net	305.47

Table 24, shows the maximum temperature at different parts of pot. Top zone has temperature close to 43°C. With new mass flow rate 8°C less temperature can be seen in outlet zone relative to 0.008 kg/s mass flow rate. Temperature in outlet zone is about 44°C.

TABLE 24: The maximum temperature at different parts of pot

Zones	Static temperature (K)
Centre	349.45
Default-interior	349.70
Inflow	349.70
Out	317.39
Plane-7	349.33
Plate	336.73
Top	316.26
Wall	349.56
Net	349.70

Figure 53, shows the cross sectional view of pot regarding to temperature distribution. Two vertical cross sectional lines are shown in this figure. It is interesting to see the effect of water outflow and how interrupts pot's symmetric situation. The cooling close to walls and top can be seen easily. Figures 54 and 55, show the temperature distribution of pot in different views, cooling of pot is the first effect of 0.005 kg/s mass flow rate, specially close to walls and top zones.

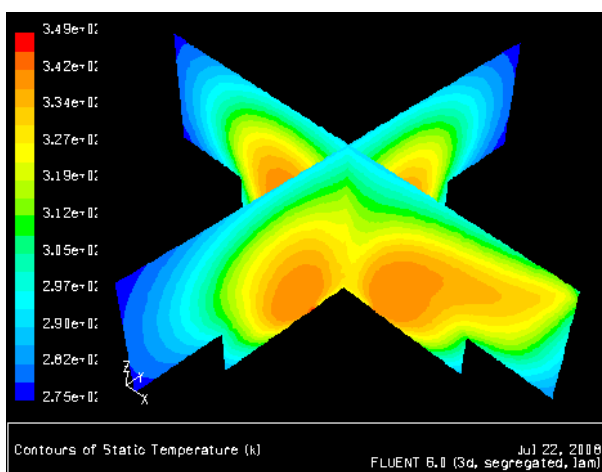


FIGURE 53: The cross sectional view of pot regarding to temperature distribution

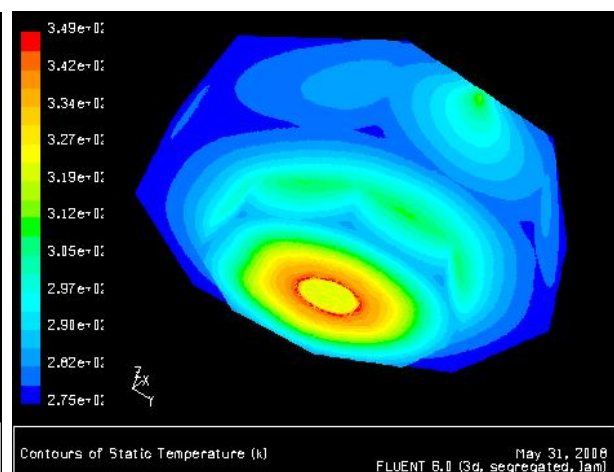


FIGURE 54: Temperature distribution in the pot

Modelling with different mass flow rates proved that temperatures in different zones of pot are sensitive to mass flow rate. This sensitivity is high in some zones. Maximum temperature in top zone equal to 329K with 0.02 kg/s mass flow rate, goes down to 310K when the mass flow rate is adjusted in 0.005 kg/s, this value is 325 K, while the mass flow rate is 0.008 kg/s.

4.6 Plate design and optimization

4.6.1 User-defined function (UDF)

A user-defined function, or UDF, is a function that user programs, that can be dynamically loaded with the FLUENT solver to enhance the standard features of the code. It can be used to define specific boundary conditions, material properties, and source terms for flow regime, as well as specify customized model parameters (e.g., DPM, multiphase models), initialize a solution, or enhance post-processing.

UDFs are written in the C programming language using any text editor and the source code file is saved with a .c extension (e.g., myudf.c). Values that are passed to a solver by a UDF or returned by the solver to a UDF are specified in SI units. Source files containing UDFs can be either interpreted or compiled in FLUENT. For interpreted UDFs, source files are interpreted and loaded directly at runtime, in a single-step process. For compiled UDFs, the process involves two separate steps. A shared object code library is first built and then it is loaded into FLUENT. Once interpreted or compiled, UDFs will become visible and selectable in FLUENT graphics panels, and can be hooked to a solver by choosing the function name in the appropriate panel. In summary, UDFs:

- Are written in the C programming language;
- Must have an include statement for the udf.h file;
- Must be defined using DEFINE macros supplied by Fluent Inc.;
- Utilize predefined macros and functions supplied by Fluent Inc. to access FLUENT solver data and perform other tasks;
- Are executed as interpreted or compiled functions;
- Are hooked to a FLUENT solver using a graphical user interface panel;
- Use and return values specified in SI units.

The C program was written to use this ability of Fluent (Appendix C). According to relation between temperature differences and heat transfer coefficient, fluent used this program to reach most accurate values for these parameters.

4.6.2 Optimization

To check most sensitive parameter, specification of tested plate has been selected as a basic, diameter of plate, gap between upper and lower plate and thickness of upper plate, were the variables that has changed within each round of modelling. Maximum outlet temperature and maximum upper plate are two very important factors from the view of safety. Results look sensitive to all changes, but plate's diameter is the most dominating parameter regarding to design criteria (not exceed more than 323 K). According to data from these modelling analysis was done to calculate diameter of plate and thickness of upper plate to fulfil design condition. The results are shown in Table 25 and Figure 56.

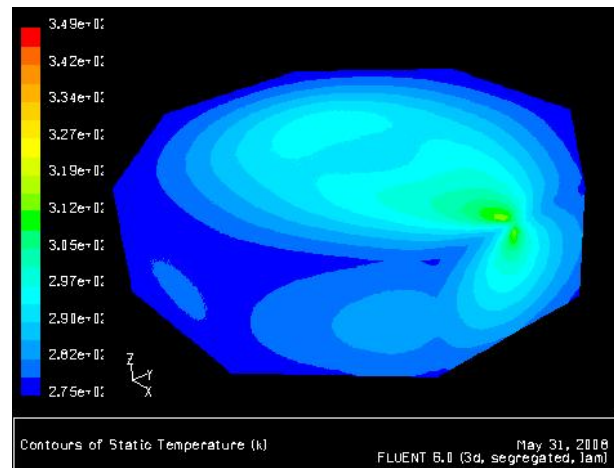


FIGURE 55: Temperature distribution in the pot

Plate with 63 cm diameter and thickness of 1.5 cm, was suggested as a final design. This size looks large at first step, but regarding to shape and size of floor in pot this design can give pleasant heat through floor to user's feet. The weight will be around 15 kg. For easy removing because of cleaning it can be built in 4 pieces. Simple linear algebra relation was applied to find the most optimum values for diameter and thickness.

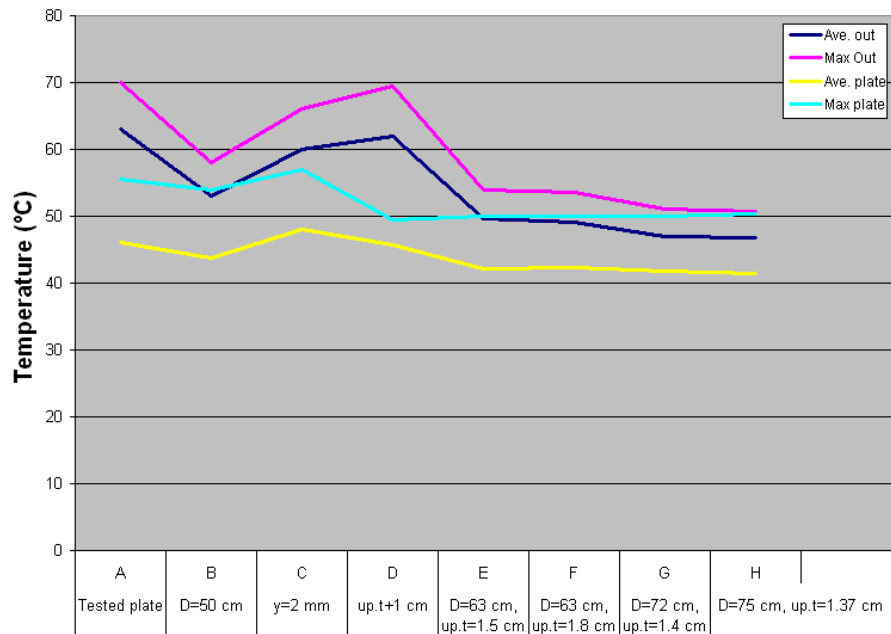


Plate with different variables

FIGURE 56: Effect of different variables of plate on temperature distribution

TABLE 25: Results of modeling for different sizes of plate

	A	B	C	E	F	G	H	I
Ave. out temp.	336	326	333	335	322.72	322.13	319.92	319.76
Max. out temp.	343	331	339	342.5	327	326.5	324	323.7
Ave. top temp.	319	316.7	321	318.8	315.21	315.3	314.77	314.49
Max. top temp.	328.5	327	330	322.5	323	323	323	323.35

A: Tested plate; B: D = 50 cm; C: y = 2 mm; E: D, upper plate + 1 cm; F: D=63, upper plate =1.5 cm, G: D=63, upper plate =1.8 cm, H: D=72, upper plate =1.4 cm, I: D=75, upper plate =1.37 cm

Type G - Plate modelling with 63 cm diameter and 1.8 cm upper plate. The plate with 63 cm diameter and 1.8 cm thickness of upper plate was selected to be modelled by Fluent. Figure 57 shows temperature distribution in the plate.

Table 26 shows heat transfer values in different zones of plate and as it can be seen the value of net heat transfer is very small, which proves that the modelling has minimum possible errors.

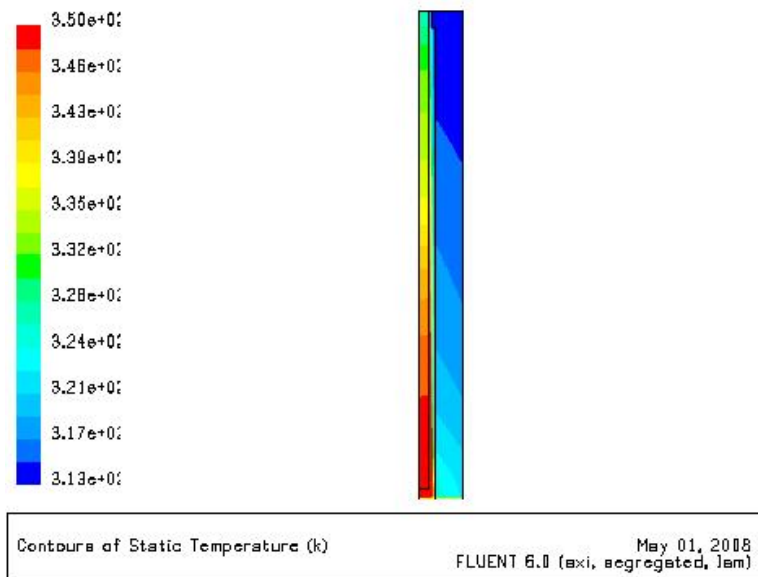
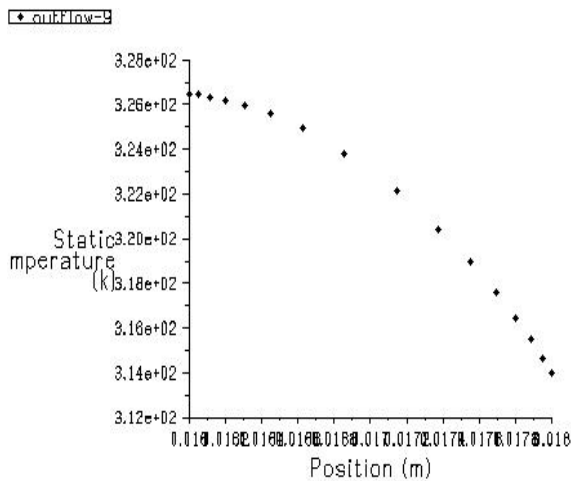


FIGURE 57: Temperature distribution in the plate – type G

TABLE 26: Heat transfer values in different zones of plate

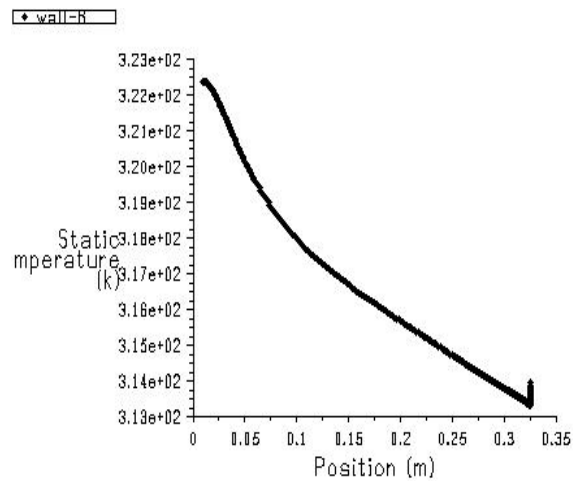
Zones	Heat flux report: W
Zone 10 (mass-flow-inlet-10)	6505.10
Zone 9 (outflow-9)	-3050.28
Zone 4 (wall)	3456.10
Zone 6 (wall-6)	0
Zone 7 (wall-7)	-407.29
Zone 8 (wall-8)	-3038.87
Zone 14 (wall-shadow)	-3455.99
Net heat-transfer	8.78

The average temperature for outflow of plate was recorded equal to 322.13 K, and for plate surface equal to 315.3 K. Figure 58 shows the temperature distribution in outflow of plate. The outflow region is the gap between upper and lower plate. Figure 59 shows the temperature distribution in upper plate of plate.



Static Temperature
FLUENT 6.0 (axi, segregated, lam) May 01, 2008

FIGURE 58: Temperature distribution in the outflow of plate

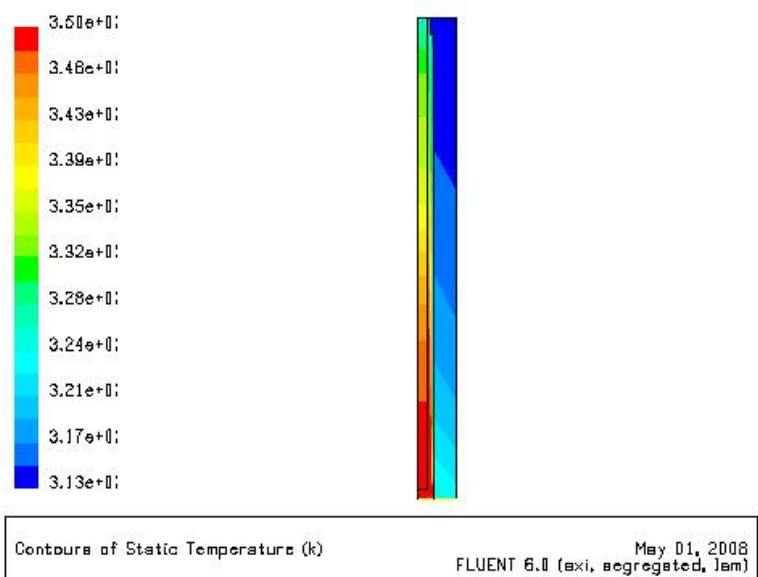


Static Temperature
FLUENT 6.0 (axi, segregated, lam) May 01, 2008

FIGURE 59: Temperature distribution in upper plate of plate

Type F - Plate modelling with 63 cm diameter and 1.5 cm upper plate. The plate with 63 cm diameter and 1.5 cm thickness of upper plate was selected to be modelled by Fluent. Figure 60 shows the temperature distribution in the plate. This model was run just to check the effect of upper plate thickness in the results. 3 mm less thickness didn't have any important change in outlet and surface temperature.

Table 27 shows heat transfer values in different zones of plate and as it can be seen the value of net heat transfer is very small, which proves



Contours of Static Temperature (k)
FLUENT 6.0 (axi, segregated, lam) May 01, 2008

FIGURE 60: Temperature distribution in the plate – type F

that the modelling has minimum possible errors. The average temperature for outflow of plate was recorded equal to 322.72 k, and for plate surface equal to 315.2 k. Figure 61 shows the temperature distribution in outflow of plate. The outflow region is the gap between upper and lower plate.

TABLE 27: Heat transfer values in different zones of plate

Zones	Heat flux report: W
Zone 7 (below)	0
Zone 6 (bs)	-412.93
Zone 10 (in)	6505.10
Zone 9 (out)	-3151.02
Zone 8 (top)	-2932.78
Zone 4 (wall)	3357.63
Zone 14 (wall-shadow)	-3357.61
Net heat-transfer	8.40

Figure 62 shows the temperature distribution in upper plate of plate.

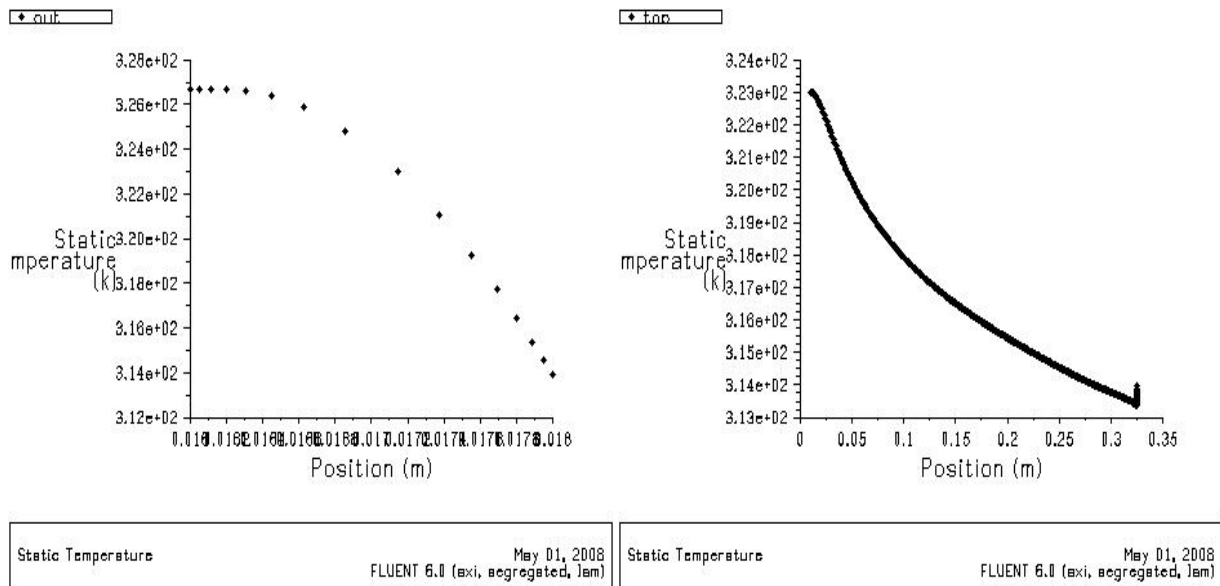


FIGURE 61: The temperature distribution in outflow of plate

FIGURE 62: Temperature distribution in upper plate of plate

Type H - Plate modeling with 72 cm diameter and 1.4 cm upper plate. According to iteration with using simple linear algebra relation, the new sizes for plate were calculated to be 72 cm for diameter and 1.4 cm for upper plate thickness. Figure 63 shows the temperature distribution in the plate. Table 28 shows heat transfer values in different zones of plate and as it can be seen the value of net heat transfer is very small, which proves that the modelling has minimum possible errors.

TABLE 28: Heat transfer values in different zones of plate

Zones	Heat flux report: W
Zone 8 (b)	0
Zone 9 (bs)	-379.39
Zone 6 (in)	6505.10
Zone 7 (out)	-2768.39
Zone 10 (top)	-3360.85
Zone 4 (wall)	3738.82
Zone 14 (wall-shadow)	-3738.19
Net heat-transfer	-2.91

The average temperature for outflow of plate was recorded equal to 319.92 k, and for plate surface equal to 314.77 k. Figure 64 shows the temperature distribution in outflow of plate. The outflow region is the gap between upper and lower plate. Figure 65 shows the temperature distribution in upper plate of plate.

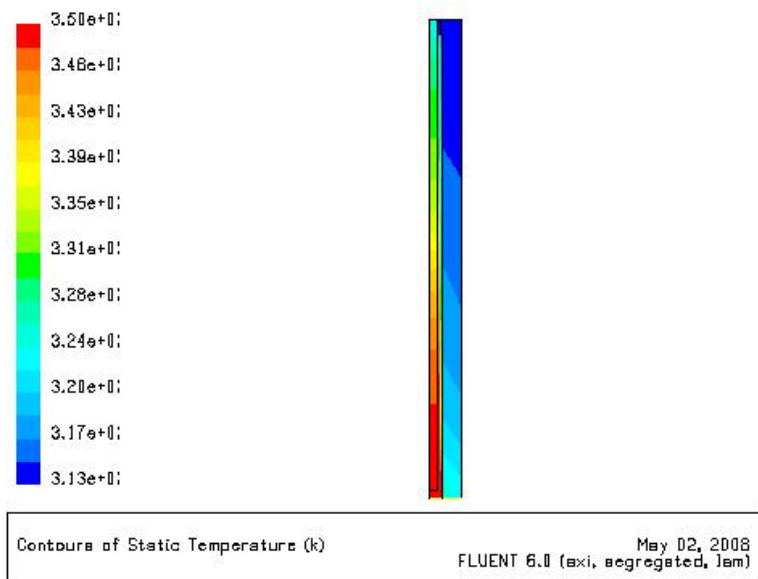


FIGURE 63: Temperature distribution in the plate – type H

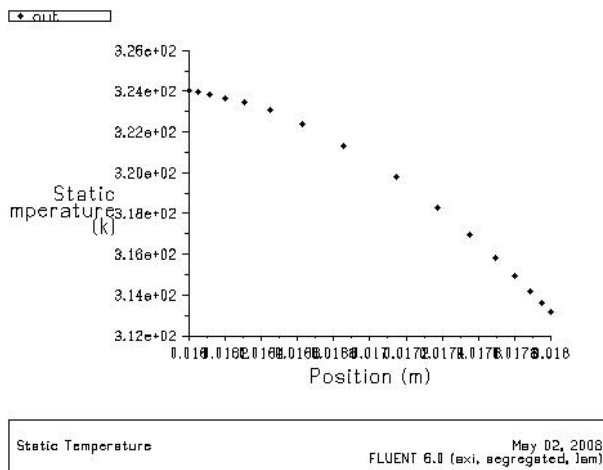


FIGURE 64: Temperature distribution in upper plate of plate

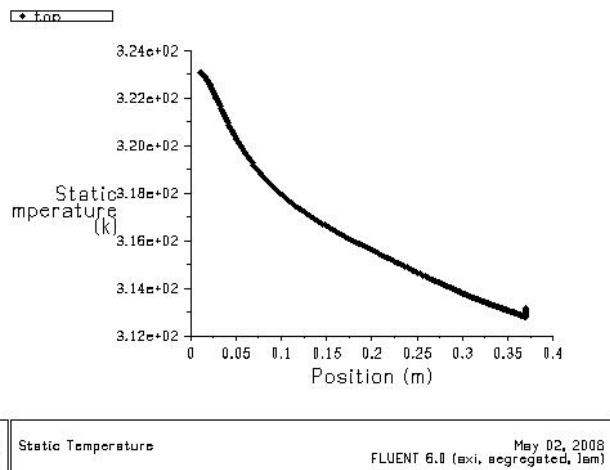


FIGURE 65: Temperature distribution in upper plate of plate

Type I - Plate modelling with 75 cm diameter and 1.3 cm upper plate. According to iteration with using simple linear algebra relation, the new sizes for plate were calculated to be 75 cm for diameter and 1.37 cm for upper plate thickness. Figure 66 shows the temperature distribution in the plate.

Table 29 shows heat transfer values in different zones of plate and as it can be seen the value of net heat transfer is very small, which proves that the modelling has minimum possible errors.

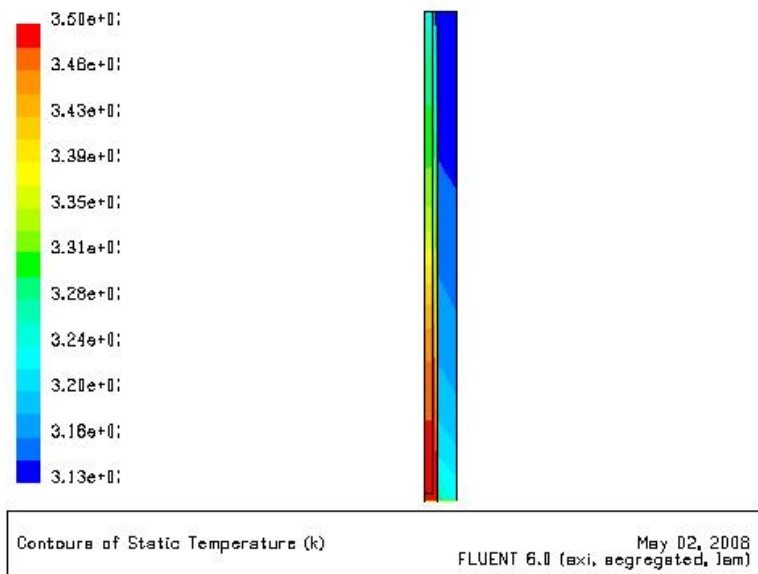
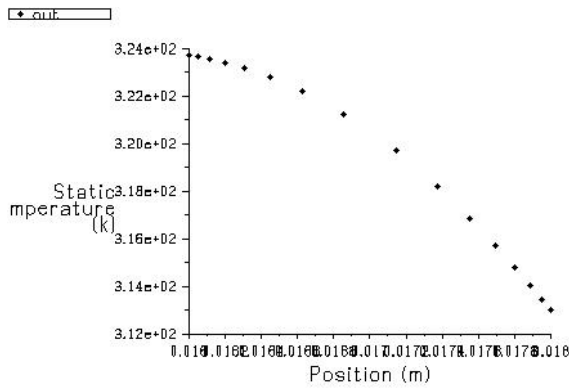


FIGURE 66: Temperature distribution in the plate type I

TABLE 29: Heat transfer values in different zones of plate.

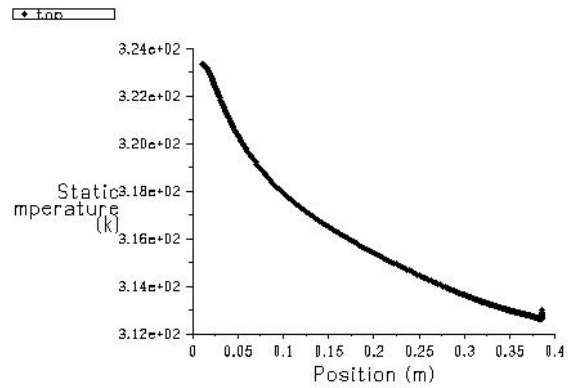
Zones	Heat Flux report: W
Zone 7 (b)	0
Zone 6 (bs)	-383.50
Zone 10 (in)	6505.10
Zone 9 (out)	-2750.77
Zone 8 (top)	-3370.01
Zone 4 (wall)	3757.54
Zone 14 (wall-shadow)	-3757.55
Net heat-transfer: 0.82	0.82

The average temperature for outflow of plate was recorded equal to 319.76 k, and for plate surface equal to 314.49 k. Figure 67 shows the temperature distribution in outflow of plate. The outflow region is the gap between upper and lower plate. Figure 68 shows the temperature distribution in upper plate of plate.



Static Temperature May 02, 2008
FLUENT 6.0 (exi, segregated, lam)

FIGURE 67: Temperature distribution in upper plate of plate



Static Temperature May 02, 2008
FLUENT 6.0 (exi, segregated, lam)

FIGURE 68: Temperature distribution in upper plate of plate

5. ECONOMY

The pot which was under monitoring had analog unit to measure mass flow rate. Then during monitoring, most reliable and accurate data were gathered in Table 30.

TABLE 30: Mass flow rates in pot during different periods

No.	Time, Date	Mass (m ³)	Duration (hours)	Mass diff. (m ³)
1	22:30, 20.12.2007	1125	17:30	3.6
	15:58, 21.12.2007	1128.6		
2	14:52, 8.3.2008	1532	51	10
	18:00, 10.3.2008	1542		
3	18:07, 10.3.2008	1542	45:40	8
	15:35, 12.3.2008	1550		
Total			114:10	21.6

Average water consumption is 4.55 m³ per 24 hours of pot's operation. This amount strongly depends on some parameters like:

- Insulation of the pot;
- Weather condition;
- Water circulation method, this item depends on family's habit and how often they cleaned their pot.

In current situation, 80°C hot water from district heating system comes to be mixed with 5°C cold water to reach 50°C desired water to pump into the pot. With simple energy balance relation and applying the conservation of mass in water mixing system according to Equation 2.7:

- m_1 = Amount of hot water from district heating system with 80°C (kg/s);
- m_2 = Amount of cold water with 5°C (kg/s);
- T_1 = Hot water temperature (80°C);
- T_2 = Cold water temperature (5°C);
- T_3 = Desired water temperature to be pumped into pot (50°C).

With simple calculation:

$$m_1 = 1.5 * m_2$$

According to this result, total of 4.55 m³ water with 50°C will be available by mixing 1.82 m³ cold and 2.73 m³ hot water with 80°C.

In measurement chapter, it was concluded that 0.03 l/s mass flow rate is sufficient, and with this flow, pot will use 1.7 m³ within 24 hours.

All measurements were done in the same location and same pot, so if there is any error because of different weather condition it has applied for both operation systems. So the errors due to different weather conditions were assumed to be negligible.

In understudy case the amount of 1 m³ hot water will be saved with using of new system in the pot. According to Orkuveita Reykjavíkur (2008), the price for hot water in Iceland is 70 ISK/ m³. So 26316 ISK will be saved within one year. With rough estimate the plate can be produced by 15000 ISK, and then the investment recovery time, can be calculated for period of less than 8 months. Also compared to the total investment cost involved in installing a spa which is around half million ISK (Normx, 2008), the investment for a new unit can be neglected.

These calculations were done according to results from experiment. This amount can be changed according to parameters which were explained previously in this chapter. But still the result looks very promising. Summary of results are illustrated in Table 31.

TABLE 31: Summary of economical comparison of tow systems

Operating type	\dot{m}_h (m³/ 24 hours)	\dot{m}_c (m³/ 24 hours)	Cost (ISK/ m³)*	Total cost (ISK)
Current system	2.73	1.82	70	191.1
Pot with plate	1.7	0	70	119
Saved per 24 hours (ISK)				72.1
Unit recovery period (Unit price/ Saved per 24 hours), (Days)				208

\dot{m}_h = Mass flow rate for hot water (m³/ 24 hours); \dot{m}_c = Mass flow rate for cold water (m³/ 24 hours); * The cost will be considered only for hot water in case of Iceland, because once cold water is in the house, there is no charge for it.

6. CONCLUSIONS

A novel approach for feeding hot water from district heating system directly into hot pots, without prior mixing with cold water has been suggested. A basic design of an open heat exchanger was made, based on a calculated and measured steady heat load requirement of 11 kW. A circular open plate heat exchanger with a dimension of 30 cm was constructed and implemented in an outdoor pool selected as a test case. Temperature field in the pool before and after implementation of the open heat exchanger was measured at different points using thermocouples. The measured temperatures were compared to thermal and fluid-dynamic simulation of the temperature and flow fields obtaining good accordance.

The results proved that in principle the open heat exchanger design works, although some design parameters need adjusting in order to meet all criteria on maximum temperature and temperature distribution in the pot. Parts of the upper plate exceeded the set maximum temperature of 50 degrees, and the water flowing out from the sides was also slightly too hot. But the pot was in fact used for days with this configuration.

More detailed measurements were made on the upper plate of the heat exchanger and detailed simulation of the heat exchanger itself was then used to obtain a value for the heat transfer coefficient for the upper plate to the surrounding water. This information was used to make an improved design for the open plate heat exchanger, stating that a diameter of 63cm and a thickness of 1.5 cm were suggested as final design. This size looks large at first step, but regarding to shape and size of floor in pot this design can give pleasant heat through floor to user's feet.

The conclusion was that for the pot used as a test case, with the heat loss and usage that was demonstrated for this particular pot, assuming a heat exchanger cost of ISK. 15000, due to improved heat efficiency, the recovery time of the investment is estimated to 8 months. In general this is a function of how the pot is used, how often the water is removed for cleaning, how long the lid is kept open etc. The maximum estimated recovery time for a pot in regular use was evaluated as 2 years.

Pressure in district heating network is enough to feed hot water into pot and pot system doesn't need pump. With installing the plate in the pot, the cold water piping will be eliminated.

REFERENCES

- A1-Arabi, M., and E1-Riedy, M.K., 1976: Natural convection heat transfer from isothermal horizontal plates of different shapes. *Int. J. Heat Mass Transfer*, 19, 1399-1404.
- Analog, 2008: Web page: www.analog.com/UploadedFiles/Data_Sheets/AD594_595.pdf
- Emeish, M.E., 2001: *Simulation of heating systems in Jordanian buildings*. University of Iceland, MSc thesis, UNU-GTP, Iceland, report 1, 91 pp.
- Fishenden, M., and Saunders, O.A., 1957: *An introduction to heat transfer*. Clarendon Press, London. 89 pp.
- Fluent, 2008: Web page: www.fluent.com.
- Fujii, T., and Imura, H., 1972: Natural convection heat transfer from a plate with arbitrary inclination. *Int. J. Heat Mass Transfer*, 15, 755-767.
- Goldstein, R.J., Sparrow E.M., and Jones, D.C., 1973: Natural convection mass transfer adjacent to horizontal plates. *Int. J. Heat Mass Transfer*, 16, 1025-1035.
- Hassan K.E., and Mohamed, S.A., 1970: Natural convection from isothermal fiat surfaces. *Int. J. Heat Mass Transfer*, 13, 1873-1886.
- Hassani, A.V., and Hollands, K.G.T., 1987: A simplified method for estimating natural convection heat transfer from bodies of arbitrary shape. Presented at the 24th National Heat Transfer Conference, Pittsburgh, Pa, *Heat Transfer*, 104, 493-500.
- Holman, J.P., 2001: *Heat transfer* (9th edition). McGraw-Hill Book Company, Singapore, 665 pp.
- Efunda, 2008: Efunda – Engineering Fundamentals, web page: www.efunda.com/formulae/heat_transfer/convection_forced/overview_forced.cfm
- Husar, R.B., and Sparrow, E.M., 1968: Patterns of free convection flow adjacent to horizontal heated surfaces. *Int. J. Heat Mass Transfer*, 11, 1206-1208.
- Ishiguro, R., Abe, T., and Nagase, H., 1977: Natural convection over heated horizontal plates (in Japanese). *Trans. Jap. Soc. Mech. Eng., Series B* 43-366, 638-645.
- ISOR, 2008: *ISOR – Iceland GeoSurvey*, web page: www.or.is.
- Kitamura, K., and Kimura, F., 1995: Heat transfer and fluid flow of natural convection adjacent to upward-facing horizontal plates. *Int. J. Heat Mass Transfer*, 38-17, 3149-3159.
- Liyod, J.R., and Moran, W.R., 1974: *Natural convection adjacent to horizontal surface of various planforms*. ASME Paper 74-WA/HT-66.
- McAdams, W.H., 1954: *Heat transmission* (3rd edition). McGraw-Hill Book Co.,NY,
- NORMX, 2008: NORMX, web page: www.normx.is.
- Olson, R.M., 1973: *Essentials of engineering fluid mechanics*. Intext Educational Publishers, NY, 637 pp.
- Pera, L., and Gebhart, B., 1973a: Natural convection boundary layer flow over horizontal and slightly inclined surfaces. *Int. J. Heat Mass Transfer*, 16, 1131-1146.

Pera, L., and Gebhart, B., 1973b: On the stability of natural convection boundary layer flow over horizontal and slightly inclined surfaces. *Int. J. Heat Mass Transfer*, 16, 1147-1163.

Perkin, P.H., 1988: *Swimming pool*. Elsevier Applied Science Ltd., London, 359 pp.

Pretota, S., Zeghmati, B., and Le Palec, G., 2000: Theoretical and experimental study of natural convection on a horizontal plate, *Applied Thermal Engineering*, 20, 873-891.

Rotem, Z., and Claassen, L., 1969: Natural convection above unconfined horizontal surfaces. *J. Fluid Mech.*, 38-1, 173-192.

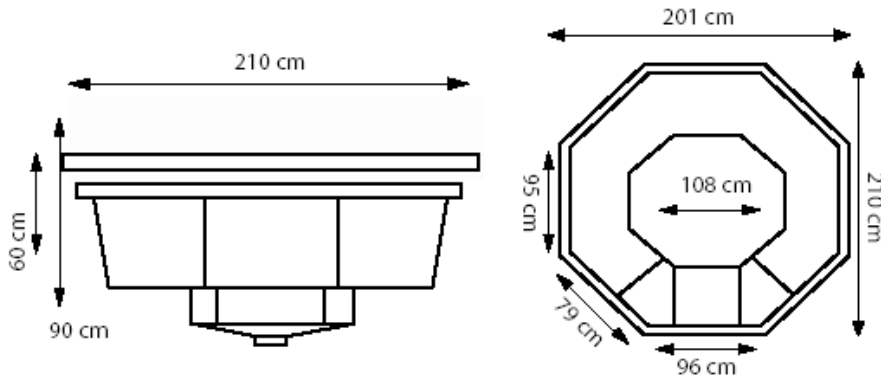
Svavarsson, G., 1990: *Designing swimming pools*. University of Iceland, B.Sc. thesis (in Icelandic), 52 pp.

Wark, K., 1988: *Thermodynamics*. McGraw-Hill Book Co., NY, 954 pp.

Wikipedia, 2008: Wikipedia, web page: en.wikipedia.org/wiki/Data_acquisition.

Yousef, W.W., Tarasuk, J.D., and McKeen, W.J., 1982: Free convection heat transfer from upward-facing isothermal horizontal surfaces. *ASME, J. Heat Trans.*, 104-3, 493-500.

APPENDIX A: THE SAMPLE OF A HOT POT



APPENDIX B: MATLAB CODE USED TO ANALYZE DATA GATHERED BY LABVIEW

```

clear all
load ap.txt
A=ap;
B=A(:,2);
L=length (B);
C=B(1:fix(L/900)*900,1);
D=zeros(9,fix(L/900)*100);
D(:)=C;
m=D;
n=zeros(9,fix(L/900));
for i=1:9,
    for j=1,
        n(i,1)=(sum(m(i,j:j+99)))/100;
    end
end
for i=1:9,
    for j=2:fix(L/900),
        n(i,j)=(sum(m(i,(100*j-99):100*j)))/100;
    end
end
plot (n')
legend ('a','b','c','d','e','h','f','air','win')
n(1,:)=n(1,:)+0.4304;
n(2,:)=n(2,:)-0.1184;
n(3,:)=n(3,:)+0.9849;
n(4,:)=n(4,:)-1.0713;

```

```

n(5,:)=n(5,)-1.3733;
n(6,:)=n(6,)-1.0816;
n(7,:)=n(7,)+0.0128;
n(8,:)=n(8,);
n(9,:)=n(9,)-0.6378;
n;

```

APPENDIX C: C PROGRAM TO CALCULATE HEAT TRANSFER COEFFICIENT

Equations:

$$h = c * (T - T_{\infty})^{1/4}$$

$$T_{\infty} = 310 \text{ k}$$

$$c = 1000$$

C Program:

```

#include "udf.h"
/*#include <math.h>*/

real C = 1000.0;
real n = 0.25;
real T_inf = 310;

DEFINE_PROFILE(free_conv_coef, t, i)
{
    real T, h;
    face_t f;
    begin_f_loop(f, t)
    {
        T = F_T(f, t);
        h = C * pow(T - T_inf, n);
        F_PROFILE(f, t, i) = h;
    }
    end_f_loop(f, t)
}
DEFINE_PROFILE(free_conv_temp, t, i)
{
    face_t f;
    begin_f_loop(f, t)
    {
        F_PROFILE(f, t, i) = T_inf;
    }
    end_f_loop(f, t)
}

```